

IV. MEDIUM-ENERGY NUCLEAR PHYSICS RESEARCH

OVERVIEW

The overall goals of the Medium-Energy Physics research program in the Argonne Physics Division are to test our understanding of the structure of hadrons and the structure of nuclei, and to develop and exploit new technologies for high-impact applications in nuclear physics as well as other national priorities. In order to test our understanding of the structure of hadrons and the structure of nuclei within the framework of quantum chromodynamics, the medium-energy research program emphasizes the study of nucleons and nuclei on a relatively short distance scale. Because the electromagnetic interaction provides an accurate, well-understood probe of these phenomena, primary emphasis is placed on experiments involving electron scattering, real photons and Drell-Yan processes.

The electron beams of the Thomas Jefferson National Accelerator Facility (TJNAF) are ideally suited for studies of nuclei at hadronic scales and represent one center of the experimental program. Staff members led in the construction of experimental facilities, serve as spokespersons or co-spokespersons for 15 experiments and are actively involved in several others. The group constructed the broad-purpose Short Orbit Spectrometer which forms half of the coincidence spectrometer pair that is the base experimental equipment in Hall C. We continue to improve the understanding of the spectrometer optics and acceptance. Argonne led the first experiment to be carried out at TJNAF in FY1996 and has completed nine other experiments.

Recently, staff members have focused increasingly on studies of the nucleon. In FY1999 measurements were made on the ratio of the electromagnetic elastic form factors of the proton using the polarization transfer method. These results confirmed the reproducibility of the surprising result that this ratio decreases substantially at high values of momentum transfer. These polarization-transfer results disagree so markedly from data recorded previously with the Rosenbluth

method, that staff members are leading a new effort to test these methods with a newly developed modified Rosenbluth technique.

Also during FY1999, measurements were performed for polarization in exclusive neutral pion photoproduction from the proton. Surprisingly, the induced-polarization was observed to oscillate strongly as a function of the reaction angle, suggesting a relatively high spin state in the proton. In FY2000, the exclusive cross sections from charged photopion production on the neutron and proton were measured up to a photon energy of 5.6 GeV as a test of “transition region” models which describe the transition from hadronic degrees of freedom to quark-gluon degrees of freedom.

Although exclusive deuteron photodisintegration experiments established that this reaction obeys quark-counting rule scaling arguments at large transverse momenta, recent complete angular distribution data recorded in FY1999 for this reaction do not support simple transition region models. Measurements of kaon production on light nuclei provide important information on the basic strangeness production mechanisms and the poorly known low energy hyperon-nucleon interaction. Pion production measurements on hydrogen, deuterium and ^3He have determined the charge form factor of the pion and have found no indication of a change in the pion field in the nuclear medium. Since the pion contains valence antiquarks, these measurements complement our high-energy Drell-Yan measurements of the antiquark distributions in nucleons and nuclei. Results of new measurements of inclusive electron scattering in the resonance region provide evidence for the concept of semi-local duality in relating averaged resonance and deep inelastic scattering yields.


HERMES, a broadly based North American-European collaboration is studying the spin structure of the nucleon using internal polarized targets in the HERA storage ring at DESY. Deep inelastic scattering has been measured with polarized electrons on polarized hydrogen, deuterium and ^3He . Argonne has concentrated on the hadron particle identification of HERMES, a unique capability compared to other spin structure experiments. In 1999 and under Argonne leadership, the dual-radiator ring imaging Cerenkov counter (RICH) was brought into operation at the design specifications to provide complete hadron identification in the experiment. The RICH has been operating routinely since its installation. This has allowed HERMES to make decisive measurements of the flavor dependence of the spin distributions. HERMES can now perform a five-component decomposition of the proton's spin structure function and can produce the first measurement of the x-dependence of the strange sea polarization. In addition, HERMES provided the first direct indications of a positive gluon spin contribution to the nucleon.

Recently, single-spin asymmetries in the azimuthal distributions of π^+ and π^0 were observed from a longitudinally polarized proton target. This new result will render transversity measurements feasible at HERMES. Now, HERMES is

poised to make the first measurements of the chiral-odd transverse structure function of the proton over the next two years. In addition, HERMES was first to observe the spin-dependent deeply virtual Compton scattering process which is an important tool for investigating the structure of the proton. Also, HERMES measured the nuclear modifications of the fragmentation function for hadrons which constrain the parton energy loss in cold nuclear matter.

Measurements of high mass virtual photon production in high-energy proton-induced reactions have determined the flavor dependence of the sea of antiquarks in the nucleon. These measurements give insight into the origin of the nucleon sea. In the same experiment, the nuclear dependence of the Drell-Yan process and the nuclear dependence of the production of heavy quark resonances such as the J/ψ and Υ have been determined. The Drell-Yan results also provide constraints on the energy loss of quarks in the nuclear medium. The heavy vector meson results provide constraints on the gluon distributions of nucleons and nuclei and a significant baseline for attempts to use heavy vector meson production as a signal of the formation of the quark-gluon plasma in relativistic heavy-ion experiments. Recently, a new initiative was approved by the FNAL PAC to continue these measurements with much higher luminosity at the FNAL Main Injector.

The technology of laser atom traps provides a unique environment for the study of nuclear and atomic systems and represents a powerful new method that is opening up exciting new opportunities in a variety of fields, including nuclear physics. The group has developed a high-efficiency, high-sensitivity magneto-optical trap for rare, unstable isotopes of krypton. The group is poised to use this method for dating ancient ground water from the Nubian aquifer in Upper Egypt. In addition, the group has trapped calcium isotopes, which is a necessary step along the way to using ^{41}Ca for radiochronology or developing a new method for measuring rates of bone loss in humans. Presently, a trap is being constructed for the purpose of measuring the charge radius of ^6He at ATLAS.



A. NUCLEON PROPERTIES

a.1 New Measurement of (G_E/G_M) for the Proton (J. Arrington, D. F. Geesaman, K. Hafidi, R. J. Holt, H. E. Jackson, D. H. Potterveld, P. E. Reimer, E. C. Schulte, K. Wijesooriya, B. Zeidman, and E01-001 Collaboration)

The structure of the proton is a matter of universal interest in nuclear and particle physics. Charge and current distributions are obtained through measurements of the electric and magnetic form factors, $G_E(Q^2)$ and $G_M(Q^2)$. These form factors can be separated by measuring elastic electron-proton scattering at two or more values of the virtual photon polarization parameter ε (*i.e.* by performing a Rosenbluth separation). Several such measurements

have been made, and global fits to these measurements¹ indicated that the ratio of G_E to G_M was consistent with unity, indicating equal distributions of charge and magnetization within the proton. Recent measurements at Jefferson Laboratory² used a recoil polarization measurement to extract G_E/G_M at large values of Q^2 . They found that the ratio of G_E/G_M was unity at low Q^2 , but fell linearly with increasing Q^2 , reaching a value of 0.3 at $Q^2 = 5.5 \text{ GeV}^2$ (see Fig. IV-1).

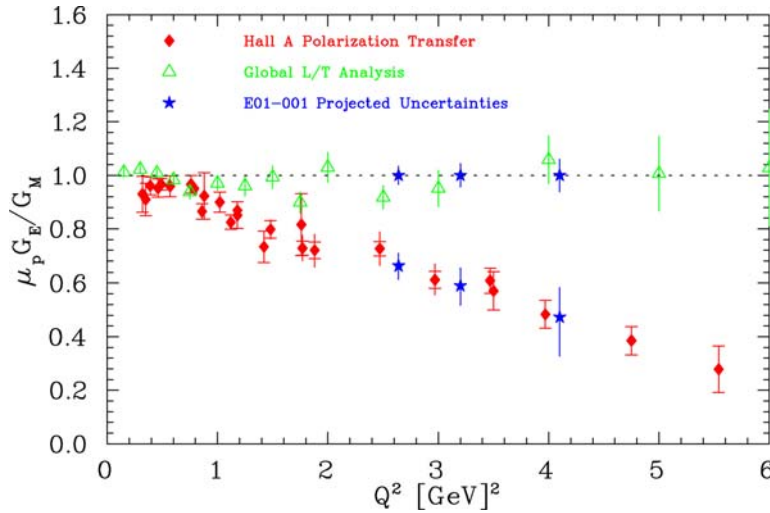


Fig. IV-1. Existing measurements of G_E/G_M , along with projected uncertainties for this experiment. There are two values shown for E01-001 at each Q^2 point. The top points show the projected uncertainty if the experiment indicates a ratio of unity, while the bottom points show the projected uncertainty if the experiment indicates the same falloff as seen by the recoil polarization measurements.

It has been suggested that the Rosenbluth data are unreliable at large Q^2 based on the fact that form factors extracted from different Rosenbluth measurements are inconsistent at large Q^2 values. We have reanalyzed the Rosenbluth measurements and find that the inconsistency between different extractions does not indicate a problem with the data or technique.³ Instead, it results from the incomplete treatment (or lack of treatment) of normalization uncertainties when data from different experiments are combined to extract the form factors. When the normalization uncertainties are properly included, or when the form factors are extracted from a single data set, the results are not inconsistent. In order to be confident in our knowledge of the proton form factors, we must determine not only

which result is correct, but also why these two techniques disagree. A systematic problem with either set of measurements would most likely affect other measurements which use the same techniques.

Experiment E01-001⁴ will perform a Rosenbluth separation to extract G_E/G_M in the range where the previous Rosenbluth data disagree with the recent measurements. The goal is to have a single data set that will provide a high-precision measurement of the ratio, with careful tests of the systematic uncertainties. In addition to careful monitoring of potential uncertainties, this measurement will use a different experimental technique which will significantly decrease our sensitivity to the systematics that have limited previous measurements.

The main difference in this measurement is that we will detect the struck proton, rather than the scattered electron. This significantly decreases almost all of the significant systematic uncertainties that have limited previous experiments. Taking data at two different ϵ values means detecting small-angle electron scattering with a high-energy beam and comparing this to large-angle electron scattering at lower energies. The result is that the measurements at large and small angles are detecting electrons with very different momenta, and are measuring cross sections that can vary by a 2-3 orders of magnitude. These measurements are therefore very sensitive to any momentum-dependent or rate-dependent effects. In addition, the cross section is very sensitive to knowledge of the scattering angle for the small angle electrons. When detecting protons, there are several advantages. There is no momentum-dependence because at fixed Q^2 , the proton momentum is constant. The cross section variation between small and large angle proton data is only a factor of 2-3, and the overall dependence of the cross section on scattering angle and beam energy is much smaller than

for the electron. Finally, the radiative corrections are smaller, and have less ϵ -dependence.

The other unusual feature of this measurement is that while we perform a Rosenbluth extraction at high- Q^2 in one spectrometer, we will make a simultaneous measurement at low Q^2 . Because the value of G_E/G_M at low Q^2 is relatively well known, and because the kinematics chosen make the low Q^2 measurement insensitive to the photon polarization ($\Delta\epsilon$ is kept small), we can use the low Q^2 point as a pseudo-luminosity monitor to correct for any error in the beam charge and target thickness measurements.

The experiment was approved for 10 days of beam time in Hall A at Jefferson Lab, and is scheduled to run in May 2002. The uncertainty in the extraction of the ratio depends on the value of G_E/G_M . Figure IV-1 shows the existing Rosenbluth and recoil polarization results, along with projected uncertainties for E01-001 for two cases: $\mu_p G_E/G_M = 1$, and $\mu_p G_E/G_M$ consistent with the polarization measurements.

¹R. C. Walker *et al.*, Phys. Rev. D **49**, 5671 (1994); P. E. Bosted, Phys. Rev. C **51**, 409 (1994)

²M. K. Jones, *et al.*, Phys. Rev. Lett. **84**, 1398 (2000); O. Gayou, *et al.*, Phys. Rev. C **64**, 038292 (2001); O. Gayou, *et al.*, Phys. Rev. Lett. **88**, 092301 (2002)

³J. Arrington, in preparation

⁴Jefferson Lab Experiment E01-001, 'New Measurement of (G_E/G_M) for the Proton', J. Arrington and R. E. Segel, spokespersons

a.2 Measurements of the Proton Elastic Electromagnetic Form Factor Ratio by Polarization Transfer (R. J. Holt, E. C. Schulte, and K. Wijesooriya, and the JLab E89-019 Collaboration)

Measurements of the ratio of the proton elastic electromagnetic form factors, $\mu_p G_{Ep}/G_{Mp}$ were performed.¹ The Jefferson Lab Hall A focal plane polarimeter was employed to measure the transverse and longitudinal components of the recoil proton polarization in electron-proton elastic scattering. The ratio of these polarization components is proportional to the ratio of the two form factors:

$$\frac{G_{Ep}}{G_{Mp}} = -\frac{P_t}{P_\ell} \frac{(E + E')}{2M_p} \tan\left(\frac{\theta_e}{2}\right)$$

where the P_i are the transverse and longitudinal components of the polarization, the E and E' are the incident and scattered electron energies, and θ_e is the electron scattering angle. The data reproduce the observation of Jones *et al.* [Phys. Rev. Lett. **84**, 1398 (2000)] that the form factor ratio decreases significantly above $Q^2 = 1 \text{ GeV}^2$ as shown in Fig. IV-2.

¹O. Gayou *et al.*, Phys. Rev. C **64** 038202 (2001)

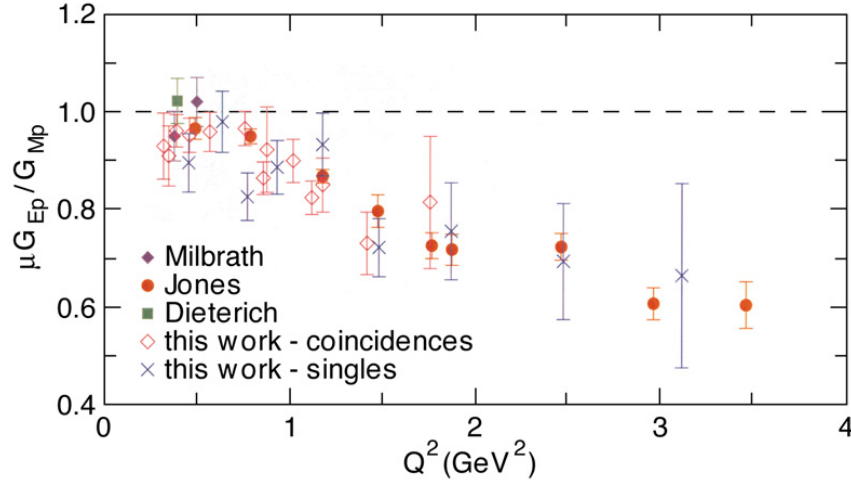


Fig. IV-2. Present results compared with the previous polarization transfer data.

a.3 Polarization Measurements in Neutral Pion Photoproduction (R. J. Holt, E. C. Schulte, and K. Wijesooriya, and JLab E94-012 Collaboration)

Measurements of the recoil polarization for the $p(\bar{\gamma}, \bar{p})\pi^0$ reaction were performed for a pion c.m. angular range of 60° to 135° and for photon energies from 0.8 to 4.0 GeV. These data represent the first polarization transfer results with circularly polarized photons measured for this reaction. The results for the induced polarization indicate much better agreement with the MAID model than the SAID model. Both models strongly disagree with the polarization transfer data.

A particularly surprising result is the observation of a strong oscillatory pattern in the angular distribution of the induced polarization at 2.5 and 3.1 GeV above the known resonance region. These results are given in Fig. IV-3. The induced polarization is related to the differential cross section $d\sigma/d\Omega$ and the differential polarization $dp/d\Omega$ by the expression

$$p_y = \frac{1}{j} \frac{dp/d\Omega}{d\sigma/d\Omega}$$

where j is the spin of the emitted proton in this case. The differential polarization can be written as

$$\frac{dp}{d\Omega} = \sum_{L=1} B_L P_L^1(\cos\theta)$$

where the B_L contain the reaction matrix elements, and assuming two amplitudes, L ranges from 1 to the sum of the angular momenta of the two amplitudes which interfere to give rise to the induced polarization. From the nature of the first associated Legendre polynomial in the equation above, the angular distribution will behave essentially like $\sin(L\theta)$. As an illustration of the strong oscillatory pattern, a $\sin(12\theta)$ curve is drawn in the figure at 2.5 GeV. The strong angular dependence noted in the data suggests an angular dependence up to $\sin(12\theta)$. This would mean that the background or a resonance contains relatively high partial waves. More finely binned data in angle and energy would be necessary to determine whether a high-spin resonance has been observed at this energy.

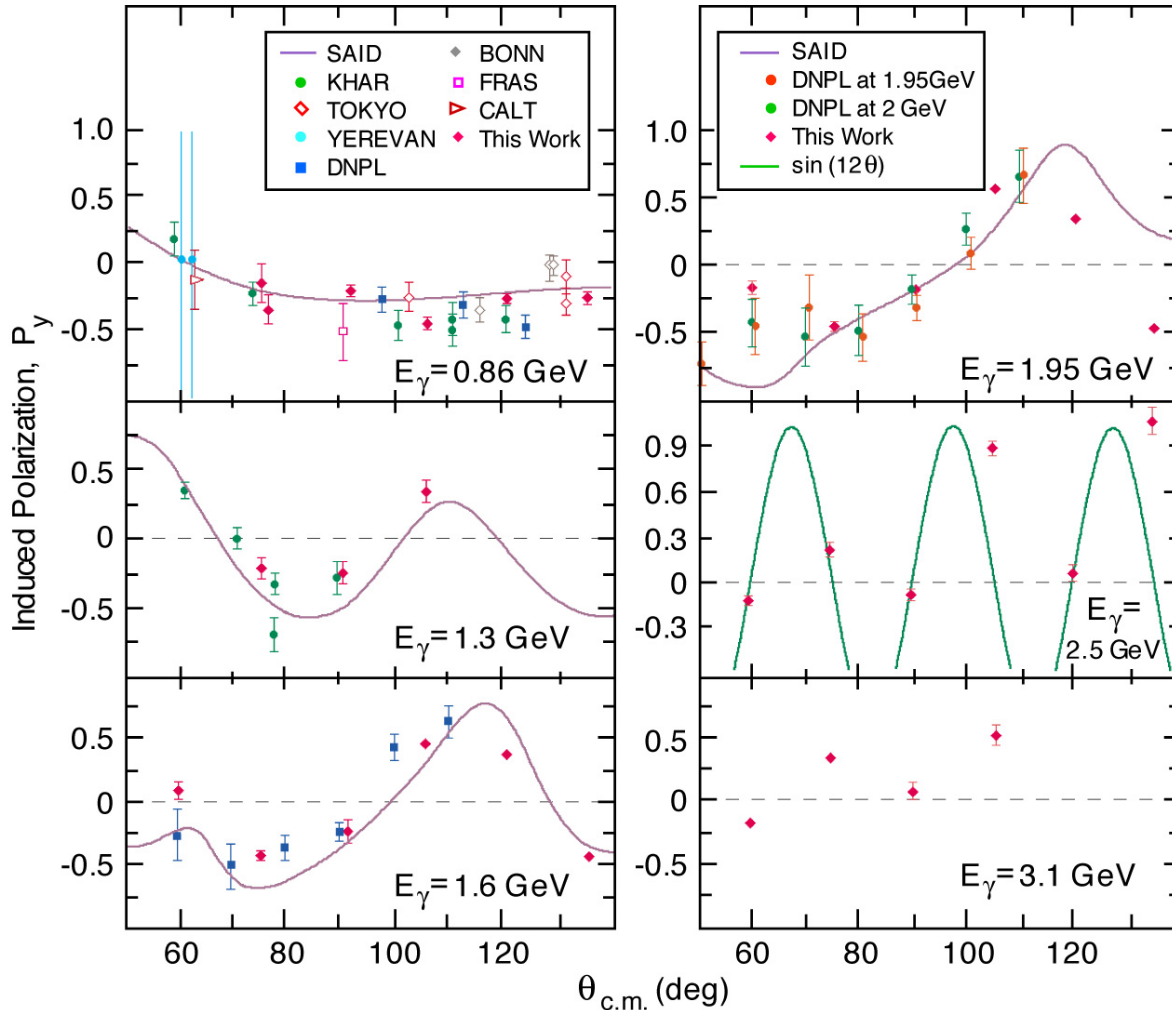


Fig. IV-3. Angular distributions of the induced polarization for neutral pion photoproduction. The $\sin(12\theta)$ curve at 2.5 GeV is drawn merely to illustrate the strong angular dependence.

a.4. Charged Pion Photoproduction from the Nucleon (R. J. Holt, J. Arrington, K. Bailey, P. E. Reimer, F. Dohrmann, K. Hafidi, T. O'Connor, E. C. Schulte, K. Wijesooriya, and JLab E94-104 Collaboration)

The goal of experiment E94-104 is to measure the cross sections for the $\gamma n \rightarrow \pi^- p$ and the $\gamma p \rightarrow \pi^+ n$ reactions for photon energies up to 5.5 GeV and at several reaction angles. The experiment was completed and the data are nearing the final analyses. From these data, the π^-/π^+ ratio can be formed and compared with existing models. One of the most celebrated models of the transition region from hadronic degrees of freedom to the quark-gluon degrees of freedom is represented by the “hand-bag” diagram. This model gives a definite prediction¹ for the ratio:

$$\frac{d\sigma(\gamma n \rightarrow \pi^- p)}{d\sigma(\gamma p \rightarrow \pi^+ n)} = \left(\frac{ue_d + se_u}{ue_u + se_d} \right)^2$$

Where the e_j are the charges of the quarks, and s and t are the usual Mandelstam variables. This model will be compared with the data over the relatively large s and t range measured in the experiment to determine whether the transition region is reached at presently available beam energies at Jefferson Lab. The data are presently undergoing analysis.

¹H. Huang and P. Kroll, Eur. Phys. J. C17, 423 (2000)

a.5. Search for QCD Oscillations in the $\gamma N \rightarrow \pi N$ Reactions (R. J. Holt, J. Arrington, D. F. Geesaman, H. E. Jackson, P. E. Reimer, K. Hafidi, E. C. Schulte, K. Wijesooriya, and JLab E02-010 Collaboration)

A proposal to search for QCD oscillations in exclusive charged photopion reactions was approved by the Jefferson Laboratory Program Advisory Committee. The goal of the experiment is to search in photopion reactions for the oscillatory effect observed in exclusive high-energy proton-proton elastic scattering. In p-p elastic scattering the cross section was found to oscillate about the $1/s^{10}$ dependence expected from the constituent counting rules. This oscillatory behavior has been ascribed¹ to a short distance (hard-scattering) amplitude which interferes with a long-distance

amplitude (Landshoff). This process is analogous to coulomb-nuclear interference observed in low energy charged particle scattering; however, the QCD oscillations arise from soft gluon radiation rather than from photon radiation as in the QED case. This interference also can give rise to polarizations observed in high energy exclusive hadron-hadron scattering processes. In the proposed experiment, the cross sections will be measured in a fine energy scan up to the highest energy available at Jefferson Lab.

¹S. J. Brodsky, C. E. Carlson, and H. Lipkin, Phys. Rev. D **20**, 2278 (1979); J. P. Ralston and B. Pire, Phys. Rev. Lett. **65**, 2343 (1990)

a.6. Separated and Unseparated Structure Functions in the Nucleon Resonance Region (J. Arrington, D. F. Geesaman, R. J. Holt, T. G. O'Neill, D. Potterveld, and E99-119, E00-002, and E00-116 Collaborations)

A great deal of our understanding of the quark structure of the nucleon comes from inclusive electron scattering. Reliable *global* descriptions of inclusive electroproduction data are necessary for electron-nucleon scattering model development, accurate radiative correction calculations, and the extraction of form factors, structure functions, and parton distribution functions from inclusive electron scattering experiments. However, most measurements have focused on the deep inelastic region. High precision cross section measurements in the resonance region, combined with a separation of the longitudinal (σ_L) and transverse (σ_T) components, will substantially improve the global description of electroproduction at moderate to high Q^2 and large Bjorken- x . While the ratio $R = \sigma_L/\sigma_T$ has been measured up to high Q^2 for elastic and deep inelastic scattering, there exist few measurements of R in the resonance region at moderate or high momentum transfers. The current uncertainty in R in the resonance region is greater than 100%. Experiment E94-110¹ ran in 1999 in Hall C at Jefferson Lab, and made a precision measurement of R in the resonance region, up to $Q^2 = 4.5 \text{ GeV}^2$. Figure IV-4

shows the preliminary results for the extraction of R as a function of W^2 for four Q^2 bins.

Previous JLab measurements of inclusive scattering in the resonance region, measuring just the F_2 structure function, have been analyzed in terms of Local Duality. It was observed that the resonance region data, when averaged over the Nachtmann variable, ξ , reproduced the structure function as measured in the deep inelastic region.² This duality of the DIS and resonance structure function held to better than 10%, down to $Q^2 = 0.5 \text{ GeV}/c^2$. It was also observed that at low ξ , the resonance region structure function deviated from the DIS value, and showed a valence-like behavior,³ going to zero as ξ decreased. While this duality has been observed for hydrogen, deuterium, and nuclear targets for F_2 , no such data existed for the F_1 structure function in the resonance region. In addition to extracting R , experiment E94-110 will also extract the separated structure functions F_1 and F_2 . These data will be used to perform tests of duality in F_1 in a similar Q^2 range to the previous F_2 measurements.

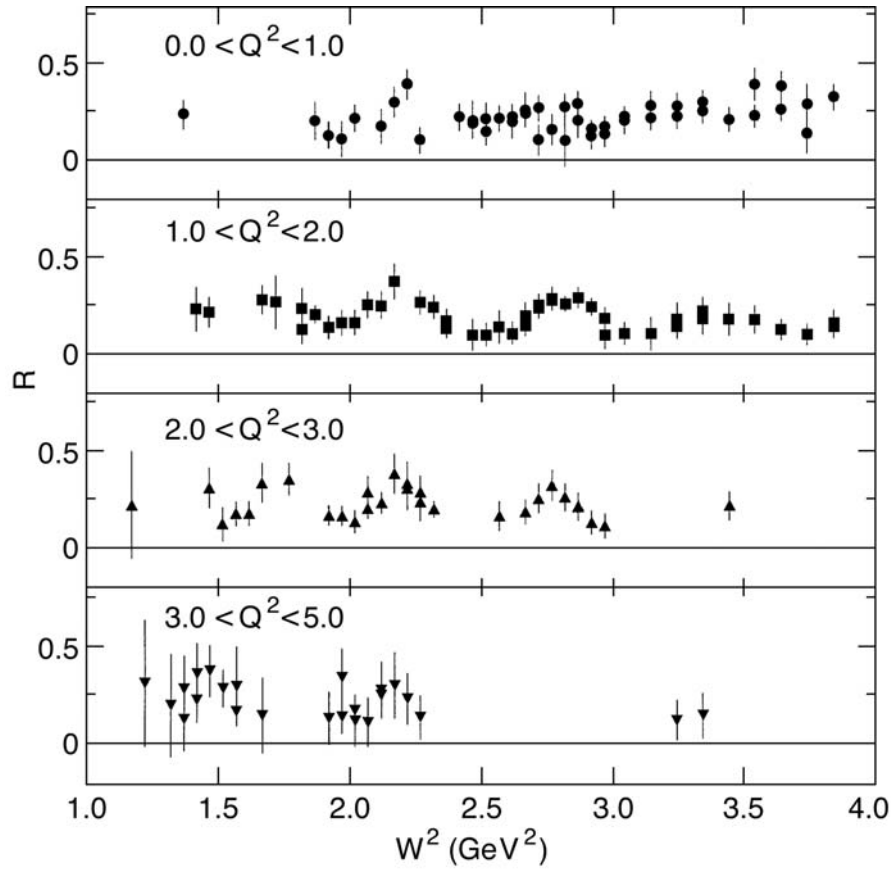


Fig. IV-4. The extracted value of $R = \sigma_L/\sigma_T$ as a function of W^2 for four Q^2 bins. These results are preliminary, and the uncertainties shown are statistical only.

Two future experiments will further extend these duality measurements. There is an approved experiment⁴ to extend duality studies on hydrogen and deuterium to $Q^2 = 7.5 \text{ GeV}^2$. Another experiment⁵ will

make additional resonance region measurements at low x and Q^2 to study the valence-like nature of the resonance region structure function.

¹JLab Experiment E94-110, "Measurement of $R = \sigma_L/\sigma_T$ in the Nucleon Resonance Region", C. E. Keppel, spokesperson

²I. Niculescu *et al.*, Phys. Rev. Lett. **85**, 1182 (2000)

³I. Niculescu *et al.*, Phys. Rev. Lett. **85**, 1186 (2000)

⁴JLab Experiment E00-002, " F_2^N at low Q^2 ", C. E. Keppel and I. Niculescu, spokespersons

⁵JLab Experiment E00-116, "Measurement of Hydrogen and Deuterium Inclusive Resonance Cross Sections at Intermediate Q^2 for Parton-Hadron Duality Studies", C. E. Keppel, spokesperson

B. SUBNUCLEONIC EFFECTS IN NUCLEI

b.1. High-Energy Angular Distribution Measurements of the Deuteron Photodisintegration Reaction (R. J. Holt, E. C. Schulte, and K. Wijesooriya, and JLab E99-008 Collaboration)

The overall goal of experiment E99-008 is to determine the mechanism which governs photoreactions in the GeV energy region. If the incoming photon couples to an interchange quark or an exchange meson, then one would expect¹ the angular distribution for the $d(\gamma,p)n$ reaction to be symmetric about 90° . If the photon couples to a nucleon or a constituent quark in the nucleon, however, one would expect^{2,3} that the differential cross section in the forward direction to be substantially larger than in the backward direction. Previous measurements⁴ extend only to a photon energy of 1.6 GeV. The previous data are consistent with the incident photon coupling to a nucleon in the deuteron. In E99-008 the angular distribution was measured from $\theta_{\text{cm}} = 30^\circ$ to 143° at photon energies between 1.6 and 2.4 GeV. The high-resolution spectrometer in Hall A was used to detect photoprotons which emerged from a

liquid deuterium target that was irradiated by bremsstrahlung photons.

Results at 1.6 and 2.4 GeV are presented in Figure IV-5. The data for E99-008 are the filled triangles presented along with the available data at the same energies from JLab experiment E89-012 (open triangles) and SLAC experiments NE8 (solid circles) and NE17 (open circles). Also presented are two angular distribution calculations for deuteron photodisintegration. The solid line is the prediction from the Asymptotic Meson Exchange (AMEC) model³ and the dashed line is the Reduced Nuclear Amplitude (RNA) prediction¹. Notice that the forward-backward asymmetry previously observed in the NE8 data (Freedman) persists up to the highest energies measured, consistent with the photon coupling to the nucleon in the deuteron.

¹S. J. Brodsky and J. R. Hiller, Phys. Rev. C **28**, 475 (1983)

²T.-S. H. Lee, Argonne National Laboratory Report No. PHY-5253-TH-88; T.-S. H. Lee, in Proceedings of the International Conference on Medium and High Energy Nuclear Physics, Taipei, Taiwan, 1988 (World Scientific, Singapore 1988), p. 563

³S. I. Nagorny, Yu. A. Kasatkin, and I. K. Kirichenkov, Sov. J. Nucl. Phys. **55**, 189 (1992)

⁴S. J. Freedman *et al.*, Phys. Rev. C **48**, 1964 (1993)

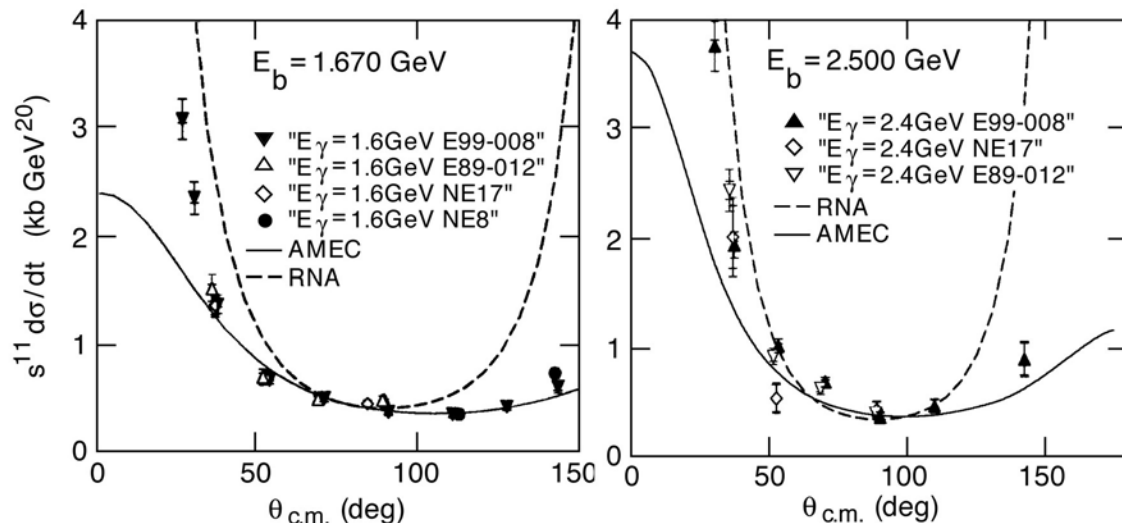


Fig. IV-5. The deuteron photodisintegration differential cross section at constant energy. Shown here are the data at 1.6 and 2.4 GeV incident photon energy, plotted as $s^{11} d\sigma/dt$, compared to previous data at forward angles. The JLab E99-008 data are the black triangles. The previous data shown are from JLab E89-012 (open triangles), SLAC NE17 (open diamonds), and SLAC NE8 (solid circles). The curves are the AMEC calculation (solid curve) and the RNA prediction (dashed curve).

b.2. Measurement of Longitudinal and Transverse Cross Sections in the ${}^3\text{He}(e,e'\pi^+){}^3\text{H}$ Reaction at $W = 1.6$ GeV (H. E. Jackson, J. Arrington, K. Bailey, D. De Schepper, D. Gaskell, D. F. Geesaman, B. Mueller, T. G. O'Neill, D. H. Potterveld, J. Reinhold, B. Zeidman, and JLab E91-003 Collaboration))

The ${}^3\text{He}(e,e'\pi^+){}^3\text{H}$ process holds much theoretical interest in that the mass-3 system is calculable using “exact” Faddeev type wave functions and hence serves as a good test of our understanding of nuclei. In addition, comparison to the fundamental $\text{H}(e,e'\pi^+)\text{n}$ process may shed some light on medium modifications to the pion electroproduction process. In general, one expects the ${}^3\text{He}(e,e'\pi^+){}^3\text{H}$ cross section to be suppressed by a factor roughly proportional to the square of the ${}^3\text{He}$ form-factor. Significant deviations from this behavior may signal changes to the pion electroproduction process in the nucleus. In experiment E91-003 at Jefferson Laboratory, the coherent ${}^3\text{He}(e,e'\pi^+){}^3\text{H}$ reaction was measured at $Q^2 = 0.4$ (GeV/c) 2 and $W = 1.6$ GeV for two values of the virtual photon polarization, ε , allowing the separation of longitudinal and transverse cross sections. The results from the coherent process on ${}^3\text{He}$ were compared to $\text{H}(e,e'\pi^+)\text{n}$ data taken at the same kinematics. This marks the first direct comparison of these processes. At these kinematics ($p_\pi = 1.1$ GeV/c), pion rescattering from the spectator nucleons in the ${}^3\text{He}(e,e'\pi^+){}^3\text{H}$ process is

expected to be small, simplifying the comparison to π^+ production from the free proton.

The unseparated and separated H and ${}^3\text{H}$ cross sections are given in Table IV-1. These cross sections are given in the laboratory frame at $Q^2 = 0.4$ (GeV/c) 2 and $\theta_{\text{pq}} = 1.72^\circ$. It is clear that both the separated and unseparated cross sections from the coherent process are, as expected, suppressed relative to the free nucleon cross section. This experiment improves upon previous ${}^3\text{H}$ experiments by measuring the cross section for a large final pion momentum such that rescattering effects should be small. Furthermore, this marks the first direct comparison of separated longitudinal and transverse ${}^3\text{He}(e,e'\pi^+){}^3\text{H}$ cross sections to those from the free proton. The results are consistent with the expectation that the suppression of the ${}^3\text{He}$ cross section relative to H is dominated by the ${}^3\text{He}$ form factor, indicating that the gross behavior of the reaction is understood and is an excellent candidate for more detailed theoretical calculation.

Table IV-1. Unseparated and separated laboratory cross sections for $\text{H}(e,e'\pi^+)\text{n}$ and ${}^3\text{He}(e,e'\pi^+){}^3\text{H}$ reactions at $W = 1.6$ GeV, $Q^2 = 0.4$ (GeV/c) 2 , and $\theta_{\text{pq}} = 1.72^\circ$. Uncertainties are statistical and systematic. A common value of the virtual photon flux Γ has been used in extracting the virtual photon cross sections to facilitate comparisons between the targets.

$d\sigma/d\Omega_\pi$ ($\mu\text{b}/\text{sr}$)		
	${}^3\text{H}$	H
Unseparated Cross Sections		
$\varepsilon = 0.490$	$14.89 \pm 0.36 \pm 1.00$	$44.23 \pm 0.36 \pm 2.52$
$\varepsilon = 0.894$	$21.80 \pm 0.40 \pm 1.50$	$58.18 \pm 0.44 \pm 3.42$
Separated Cross Sections		
σ_L	$17.12 \pm 1.36 \pm 2.38$	$34.57 \pm 1.41 \pm 4.38$
σ_T	$6.50 \pm 0.95 \pm 1.45$	$27.29 \pm 0.96 \pm 2.89$

b.3. Electroproduction of Kaons and Light Hypernuclei (J. Arrington, K. Bailey, F. Dohrmann, D. F. Geesaman, K. Hafidi, H. E. Jackson, B. Mueller, T. G. O'Neill, D. Potterveld, P. Reimer, B. Zeidman, and E91-016 Collaboration)

Jefferson Lab experiment E91-016, “Electroproduction of Kaons and Light Hypernuclei”, is a study of the production of Kaons on targets of H, D, ^3He , and ^4He at an incident electron energy of 3.245 GeV and $Q^2 \approx 0.37 \text{ GeV}^2$. For H and D targets, additional data were obtained at an energy of 2.445 GeV and $Q^2 \approx 0.5 \text{ GeV}^2$. The scattered electrons and emergent K^+ were detected in coincidence with the use of the HMS and SOS spectrometers in Hall C. Particle identification utilizing time-of-flight techniques together with Aerogel Cerenkov detectors provided clean missing-mass spectra and allowed subtraction of random backgrounds. In addition to obtaining spectra, angular distributions were measured at forward angles with respect to the virtual photons.

The fundamental interaction being studied is the $N(e,eK^+)Y$ where Y is either a Λ or Σ and N is a nucleon, either free or bound in a nucleus. For H, the final state can only be a Λ or Σ^0 , with a missing mass spectrum consisting of two distinct peaks. For heavier targets, however, not only can Σ^- be produced on the neutron, but the relative motion of the bound nucleons results in quasi-free broadening of the peaks, as is illustrated in Fig. IV-6. Since there is no known bound state in the mass 2 hyper-nuclear system, only quasi-free production is observed. For D, the Fermi broadening is less than the mass difference between hyperons so that separation of the Λ and Σ contributions utilizing Monte-Carlo simulations that include final-state-interactions, FSI, is relatively straightforward. Because of the small mass difference between Σ^0 and Σ , however, distinguishing between these contributions is not possible without assuming that the Λ/Σ^0 ratio is the same as that for the free proton. Subtraction of the normalized Σ^0 contribution yields a value for Σ^- production on the neutron. The ratio of cross sections for Σ^0/Σ^- suggests s-channel dominance for the $D(e,eK^+)$ reaction in the present kinematic regime.

For the heavier targets, $^3,^4\text{He}$, both Fermi broadening and a rapidly increasing number of final state configurations make it more difficult to separate the various contributions, as is evident in the figure. Indeed, there is no obvious indication of the Σ contributions for ^4He . As a result, the simulations are sensitive to detailed descriptions of the wave functions and final configurations for these nuclei. The simulations utilize various forms for the momentum distributions within the target nuclei, but there is

qualitative agreement for the shapes of the quasi-free distributions. The detailed fits require FSI and small variations in shape near the quasi-free threshold that make it difficult to extract precise cross sections for formation of bound states. Nevertheless, the analyses of the data for ^4He provide unambiguous evidence (Fig. IV-6) for the formation of the bound hypernucleus hyper- ^4H ; the first observation of electroproduction of a hyper-nuclear bound state. From other reactions, a 1^+ excited state bound by approximately 1 MeV is known to exist in this nucleus; the 0^+ ground state is bound by 2.04 MeV. The evidence for the electroproduction of the hypertriton, *i.e.*, the p-n- Λ bound state known to have a binding energy of approximately 130 keV, is less convincing. While barely discernible near zero degrees, the bound state becomes more evident away from 0 degrees, inasmuch as the quasifree peak moves to higher missing mass.

Extraction of cross sections for specific channels becomes more difficult with increasing mass because of the rapidly growing number of possible final configurations. As is seen in the figure, however, the various models that have been utilized for the Helium isotopes yield simulations that are in reasonable agreement with the shapes of the spectra. Since it is not possible to distinguish between Σ^0 and Σ^- production, the analyses assume the Λ/Σ^0 ratio data for H obtained at the same laboratory settings as input to extract the Σ^- yields. Further analyses of these results are in progress. There are suggestions of peaks in the missing mass regions near the Σ threshold. Inasmuch as there are issues related to detailed configurations, however, there is no plausible evidence for possible bound Σ states at this time.

E91-016 is a high-statistics study of Kaon electroproduction on light nuclei. During the course of the experiment, extensive data were obtained for the H target as well as additional calibration data for C and Al. These latter data have been analyzed in a relatively crude manner to ascertain the general mass dependence of the cross sections for Kaon electroproduction. Other aspects of the experiment, such as Omega production on the proton, will be reported later. E91-016 has provided all or a substantial fraction of the thesis data for students from Hampton University, University of Pennsylvania, and Temple University.

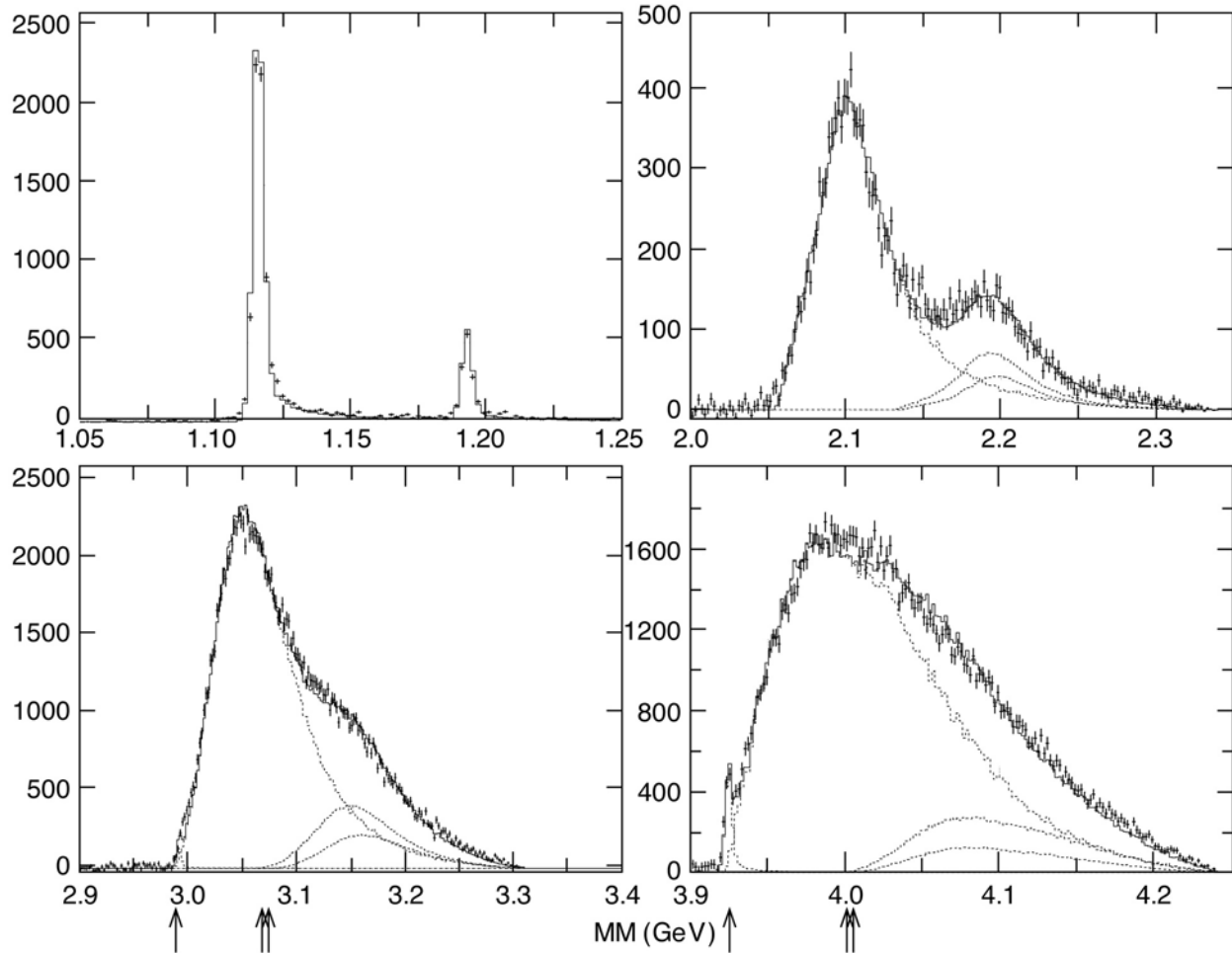


Fig. IV-6. Spectra obtained along the virtual photon direction for the $A(e,e'K^+)YX$ reaction where A is H , D , ${}^3\text{He}$, and ${}^4\text{He}$ (upper left, upper right, lower left, lower right, respectively) while X represents the residual system. The dotted curves indicate Monte-Carlo simulations for Λ , Σ^0 , and Σ^- production as well as possible bound-states; the solid curves are the sums of these individual contributions. The arrows indicate the thresholds for quasi-free Λ , Σ^0 , Σ^- production on ${}^3\text{He}$ and ${}^4\text{He}$.

b.4. Measurements of the Nuclear Dependence of $R = \sigma_L/\sigma_T$ at Low Q^2 (J. Arrington, D. F. Geesaman, T. G. O'Neill, D. Potterveld, and the JLab E99-118 Collaboration)

Inclusive electron scattering is a well-understood probe of the partonic structure of nucleons and nuclei. Deep inelastic scattering has been used to make precise measurements of nuclear structure functions over a wide range in x and Q^2 . The ratio $R = \sigma_L/\sigma_T$ has been measured reasonably well in deep inelastic scattering at moderate and high Q^2 using hydrogen and deuterium targets. However, R is still one of the most poorly understood quantities measured in deep inelastic scattering and few measurements exist at low Q^2 or for nuclear targets. Existing data at moderate to large values of Q^2 rule out significant nuclear effects in R .

Jefferson Lab Experiment E99-119 is a direct measurement of R at low x and low Q^2 . The experiment was performed in July of 2000 and recorded data on hydrogen, deuterium, and heavier nuclei. Because the data extend to very low x and Q^2 , the radiative corrections become extremely large and need to be modeled carefully. The analysis is still underway and is currently focused on testing the radiative corrections to determine how low in Q^2 the cross section can be reliably extracted. Final results are expected in the next year.

b.5. Measurement of the EMC Effect in Very Light Nuclei (J. Arrington, F. Dohrmann, D. Gaskell, D. F. Geesaman, K. Hafidi, R. J. Holt, H. E. Jackson, D. H. Potterveld, P. E. Reimer, B. Zeidman, and E00-101 Collaboration)

The EMC collaboration first measured the difference between the structure function of heavy nuclei and deuterium, indicating a modification of the quark distributions in the nuclear environment. They observed a suppression of the structure function in heavy nuclei at large values of x (corresponding to large quark momenta), and an enhancement at low x values. The EMC effect was subsequently measured by several other experiments for a variety of nuclei. The ratio of F_2 for the heavy nucleus to F_2 for the deuteron has the same shape for all nuclei, and only the magnitude of the enhancement and suppression depends on the nucleus. Many attempts have been made to explain the EMC effect, but none can fully reproduce the observed modifications, and there is still no consensus on which effect or combination (if any) explains the data.

The EMC effect for ${}^3\text{He}$ and ${}^4\text{He}$ experiment E00-101¹ will be measured. The current data cannot distinguish different models of the density dependence of the effect. By measuring the EMC effect for light nuclei (${}^3\text{He}$ and ${}^4\text{He}$) we will extend the range of nuclei for which precision data exists. Because ${}^4\text{He}$ has an anomalously large density for a light nucleus, it is the most sensitive test to determine if the EMC effect scales with A or with nuclear density. More importantly, we will take precision data that can be

compared to exact few body calculations. If the EMC effect is caused by few nucleon interactions, the universal shape in heavy nuclei may be a result of a saturation of the effect, and the shape may be different in few-body nuclei. Figure IV-7 shows the existing data on ${}^3\text{He}$, along with the projected uncertainties for the E00-101 measurement. The curves show calculations of the EMC effect for ${}^3\text{He}$ and ${}^4\text{He}$, along with the fit to the data from heavy nuclei. While the existing data on heavy nuclei all show the same x -dependence, these calculations predict significantly different dependences for very light nuclei. E00-101 will be able to measure these differences, and allow us to distinguish between different models of the EMC effect based on their predictions for few-body nuclei.

Finally, a measurement of $A \leq 4$ nuclei will provide a way to test models of nuclear effects in light nuclei. Models of the nuclear effects in deuterium and ${}^3\text{He}$ must be used to extract information on neutron structure, so we need to be able to test and evaluate these models. A high precision measurement including ${}^1\text{H}$, ${}^2\text{H}$, ${}^3\text{He}$, and ${}^4\text{He}$ will give a single set of data that can be used to evaluate these models in several light nuclei, and help quantify the model dependence of the neutron structure functions inferred from measurements on ${}^2\text{H}$ and ${}^3\text{He}$.

¹Jefferson Lab Experiment E00-101, "A Precise Measurement of the Nuclear Dependence of Structure Functions in Light Nuclei", J. Arrington, spokesperson

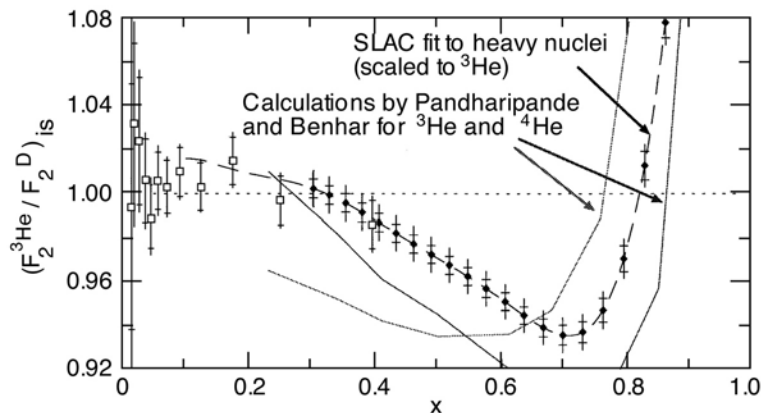


Fig.IV-7. Existing data for the EMC effect in ${}^3\text{He}$ from the HERMES experiment (hollow squares), along with projected uncertainties for the E00-101 measurement. The solid lines are calculations for ${}^3\text{He}$ and ${}^4\text{He}$, while the dashed line is the SLAC fit to the EMC effect in heavy nuclei.

b.6. Measurement of High Momentum Nucleons in Nuclei and Short Range Correlations
(J. Arrington, D. F. Geesaman, K. Hafidi, R. J. Holt, H. E. Jackson, P. E. Reimer,
E. C. Schulte and JLab E02-019 Collaboration)

Inclusive scattering from nuclei at low energy transfer (corresponding to $x > 1$) is dominated by quasielastic scattering from nucleons within the nucleus. As the energy transfer is decreased, the scattering probes nucleons of increasing momentum and we can map out the distribution of high momentum nucleons in nuclei. Experiment E89-008¹ measured inclusive scattering for deuterium, carbon, iron, and gold at $x > 1$ using 4 GeV electrons at Jefferson Lab. These data can be used to constrain the high momentum components of nuclear spectral functions. In addition, as the high momentum nucleons are dominantly generated by short-range correlations (SRCs), these data allow us to examine the strength of two-nucleon correlations in heavy nuclei.

Experiment E02-019² will extend these measurements to higher values of x and Q^2 using the 6 GeV electron beam at JLab. In addition to measuring scattering from deuterium and heavy nuclei, data will be taken on ^3He and ^4He . The higher Q^2 values in this experiment should simplify the extraction of the high momentum components, as effects such as final state interactions should be reduced as Q^2 is increased. Measurements with few-body nuclei (^2H , ^3He , and ^4He) allow contact with theoretical calculations *via* essentially “exact” calculations for few-body systems. This can be used to study in detail contributions to the interaction beyond the impulse approximation (*e.g.* final state interactions). Data on heavy nuclei can then be used to constrain the high momentum components of their spectral functions, as well as allowing an extrapolation nuclear matter.

The extension to higher energies will provide us with significantly greater sensitivity to the high momentum components of the nuclear wave function, probing nucleons with momenta in excess of 1000 MeV/c. This will improve our ability to study the structure of nucleon correlations in nuclei. Direct comparisons of heavy nuclei to deuterium at large x will allow us to map out the strength of two-nucleon correlations in both light and heavy nuclei. In addition, comparing heavy nuclei and ^3He at extremely large x values ($2.5 <$

$x < 3$) may provide the first experimental signature of multi-nucleon correlations. In this region, the contribution from two-nucleon short-range correlations (SRCs) should be small, and multi-nucleon correlations may dominate the momentum distribution. This would be a first step in the study of multi-nucleon correlations. These correlations are important because they are an integral part of the structure of nuclei, but also because they represent local configurations of extremely high density within the nucleus.

In addition to probing nucleon distributions and short range correlations, these data fill a significant void in our knowledge of the nuclear structure function. Little data exist for nuclei at large x , yet such data are important in the study of scaling and duality, higher twist effects, and nuclear dependence of the structure function. In addition, while the $x > 1$ structure function is often neglected, it must be included in studies of the energy-momentum sum rule or analysis of the QCD moments. While E02-019 will focus on the study of the high momentum nucleons in nuclei, it provides the data necessary for a variety of studies.

The experiment was approved by PAC21 for 28 days of beam time in Hall C with an A- scientific rating. Figure IV-8 shows the coverage of the proposed measurement compared to existing data from JLab E89-008 and SLAC-NE3. Over the entire x range, there is a significant increase in the Q^2 coverage compared to previous experiments. The data in the scaling region (above $Q^2 \sim 3 \text{ GeV}/c^2$) are especially important, as this is the region where final state interactions appear to be small. In the range of $1.5 < x < 2$ the sensitivity of the data to two-nucleon correlations is greatest, and we will increase not only the Q^2 range, but also add the helium isotopes to better study the A-dependence of the SRCs. For $2.5 < x < 3$, we will take the first high precision data in the scaling region, which will provide a much greater sensitivity to the presence of multi-nucleon correlations.

¹J. Arrington, *et al.*, Phys. Rev. Lett. **82**, 2056 (1999)

²Jefferson Lab Experiment E02-019, “Inclusive Scattering from Nuclei at $x > 1$ and High Q^2 with a 6 GeV Beam”, J. Arrington, D. B. Day, A. Lung, and B. W. Filippone spokespersons

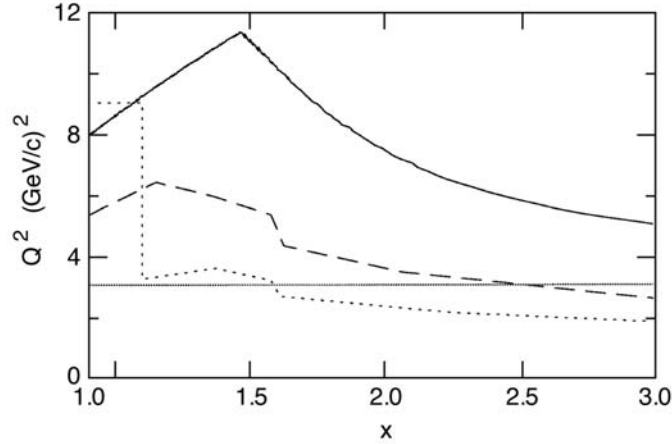


Fig. IV-8. Kinematic coverage in x and Q^2 for the proposed measurement (solid line) compared to the previous JLab (dashed) and SLAC (dotted) data. The horizontal line at $Q^2 = 3$ indicates the region where the current data show the onset of scaling.

b.7. Search for the Onset of Color Transparency (Letter of Intent LOI-02-004 to JLab-PAC21) (K. Hafidi, B. Mustapha, J. Arrington, F. Dohrmann, A. El Alaoui, D. F. Geesaman, R. J. Holt, H. E. Jackson, D. Potterveld, P. Reimer, E. C. Schulte and Hall B Collaboration)

According to QCD, pointlike colorless systems, such as those produced in exclusive process at high Q^2 have a vanishingly small transverse size. Therefore, they are expected to travel through nuclear matter experiencing very little attenuation. This effect, referred to as color transparency (CT), cannot be explained in the hadronic picture of nuclear matter (Glauber theory) and calls upon the quark's degrees of freedom. Earlier measurements were mainly focused on quasi-elastic hadronic (p , $2p$) and leptonic ($e,e'p$) scattering off nuclear targets. Although high energy experiments (Fermilab E791)¹ observed a clear signal of CT, none of the intermediate energy experiments (SLAC² and JLab³) produced an evidence for CT up to a $Q^2 \sim 8 \text{ GeV}^2$

In this experiment, we propose to look for CT in the incoherent diffractive ρ^0 electroproduction on hydrogen (or deuterium), carbon and copper. In this process, the virtual photon fluctuating into a $q\bar{q}$ pair could produce a vector meson by interacting with a nucleon inside the target, see Fig. IV-9. This fluctuation can propagate over a distance ℓ_c called "coherence length".

The observable carrying the signature of CT is the transparency ratio:

$$T_A = \frac{\rho_A}{A\rho_N}$$

where ρ_A is the ρ^0 production cross section on the nuclear target (A) and ρ^0 is measured on the nucleon. The possible manifestation of CT is a significant increase of T_A as a function of Q^2 . Recent theoretical calculations by Kopeliovich *et al.*⁴ predicted an increase of more than 40% at $Q^2 \sim 4 \text{ GeV}^2$, see Fig. IV-9.

Recent measurements by HERMES⁵ have shown that T_A increases when ℓ_c varies from long to short compared to the size of the nucleus. This so-called coherence length effect can mock the signal of CT and should be under control. Therefore, we propose to measure the Q^2 dependence of the transparency T_A at fixed coherence length ℓ_c . Figure IV-10 shows the proposed measurements at complementary ℓ_c values to map the whole Q^2 region up to 4 GeV^2 .

¹E. M. Aitala *et al.*, Phys. Rev. Lett. **86**, 4773 (2001)

²N. C. R. Makins *et al.*, Phys. Rev. Lett. **72**, 1986 (1994); T. G. O'Neill *et al.*, Phys. Lett B **351**, 87 (1995)

³D. Abbott *et al.*, Phys. Rev. Lett. **80**, 5072 (1998); M. Battaglieri *et al.*, Phys. Rev. Lett. **87**, 172002 (2001)

⁴B. Kopeliovich *et al.*, Phys. Rev. C **65**, 035201 (2002)

⁵K. Ackerstaff *et al.*, Phys. Rev. Lett. **82**, 3025 (1999)

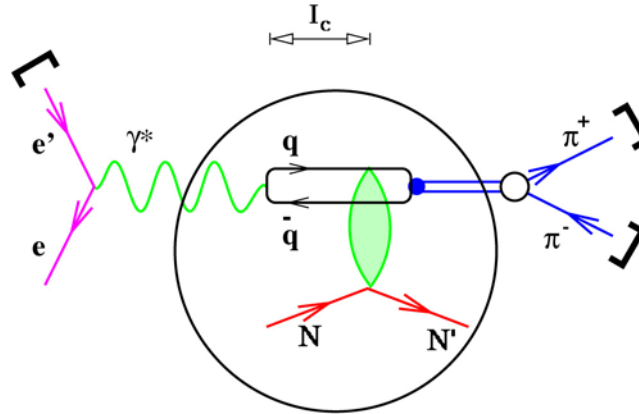


Fig. IV-9. Exclusive electroproduction of the ρ^0 meson.

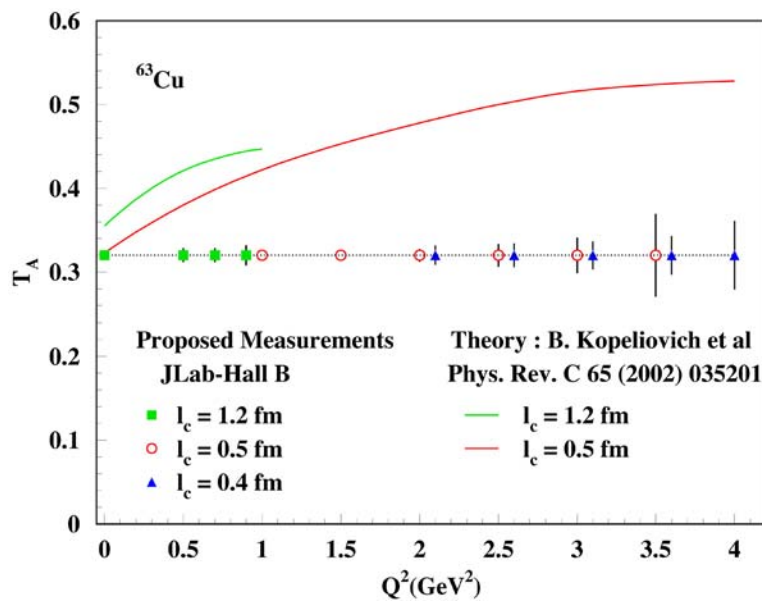


Fig. IV-10. Theoretical predictions and simulated results

b.8. Measurement of the Transparency Ratio for the $A(\gamma, \pi^- p)$ Reaction in Helium and Deuterium (R. J. Holt, J. Arrington, K. Bailey, P. E. Reimer, F. Dohrmann, K. Hafidi, T. O'Connor, E. C. Schulte, and K. Wijesooriya, and JLab E94-104 Collaboration)

The transparency for the ${}^4\text{He}(\gamma, \pi^- p)$ reaction compared with the $\text{D}(\gamma, \pi^- p)$ reaction was measured as a function of photon energy in Hall A at Jefferson Laboratory. The fundamental process $\gamma n \rightarrow \pi^- p$ exhibits a scaling behavior consistent with the constituent counting rules above a photon energy of 2.5 GeV. Thus, one can use

this reaction in the nuclear medium to determine whether the onset of color transparency has been observed. The pion is expected¹ to exhibit the phenomenon of color transparency more readily than the proton since the pion has only two constituent partons. The data are presently being analyzed.

¹B. Blättel *et al*, Phys. Rev. Lett. **70**, 896 (1993)

b.9. New Optics and Acceptance Model for the Jefferson Lab High Resolution Spectrometers (J. Arrington, O. Okafor, D. H. Potterveld and E. C. Schulte, M. Boswell,* R. Ent,* and D. Meekins*)

The standard equipment for Hall A at Jefferson Lab consists of a pair of nearly identical high resolution spectrometers (HRS). While these spectrometers provide a very good measurement of the momentum of detected particles, the optics models that have been used in the past did not accurately reproduce the acceptance of the spectrometer. Experiments that needed to extract a cross section have thus been forced to adjust the apertures in the model to reproduce the data (replacing physical apertures with effective ones), or apply cuts to the data to the region of uniform acceptance.

Experiment E99-008, a measurement of the angular distribution of deuteron photodisintegration, was performed in Hall A using the HRS spectrometers. To avoid applying cuts that would have significantly reduced the statistics of the measurements, a new optics and acceptance model was generated for this and future experiments. The new model uses COSY generated

transformations to model the magnetic elements, and applies cuts for the collimator, apertures within each of the magnets, and the active region of the detectors. The spectrometer model was incorporated into SIMC, the physics simulation code used by several experiments in Hall C. The new spectrometer model did a better job of reproducing the data, improving the acceptance of the spectrometer. The new HRS model is currently being incorporated into the standard Hall A physics simulation code, MCEEP, so that the new model can be evaluated more carefully and be used in the analysis of other experiments. While this new model fixes the obvious discrepancies between the old model and the data, there are still small differences in the distribution of events at the detector plane. We are currently working to optimize the optics model by including small position offsets and rotations of the magnets to reproduce the distortions observed in the event distributions at the detectors.

*Jefferson Laboratory

C. QUARK STRUCTURE OF MATTER

c.1. Measurement of the Structure Function of the Pion (R. J. Holt, P. E. Reimer, and K. Wijesooriya)

The light mesons have a central role in nucleon and in nuclear structure. The masses of the lightest hadrons, the mesons, are believed to arise from chiral symmetry breaking. The pion, being the lightest meson, is particularly interesting not only because of its importance in effective theories, but also because of its importance in explaining the quark sea in the nucleon and the nuclear force in nuclei.

Until recently, the pion structure function was only studied *via* πp Drell-Yan scattering. The analysis of the Drell-Yan data was questioned¹ recently, and now studies of this analysis are underway. New measurements² at a very low momentum fraction, x , have been made with semi-inclusive deep inelastic

scattering through the process $ep \rightarrow e'NX$. In this reaction, the virtual photon scatters off of the pion in the $|\pi^+n\rangle$ or $|\pi^0p\rangle$ or Fock components of the proton and the intact nucleon is detected.

Studies are underway of the feasibility of making such measurements at Jefferson Lab using an 11-GeV incident electron beam using a modified RAPGAP³ Monte Carlo program. Early results show that the relatively high luminosity which can be achieved at an upgraded Jefferson Lab will enable the pion structure to be measured, over a limited range in x . Additional investigations are being made of this reaction using a future electron-ion collider.⁴

¹M. B. Hecht *et al.*, Phys. Rev. C **63**, 025213 (2001)

²C. Adloff *et al.* (H1 Collaboration, Eur. Phys. J. C **6**, 587 (1999)

³H. Jung, Comp. Phys. Commun. **86**, 147 (1995)

⁴R. J. Holt and P. E. Reimer, Proc. of the Second Workshop on the Polarized Electron Ion Collider, MIT (2000)

c.2. Measurements of Spin-Structure Functions and Semi-Inclusive Asymmetries for the Nucleon at HERA (H. E. Jackson, A. El Alaoui, K. G. Bailey, T. P. O'Connor, K. Hafidi, D. H. Potterveld, P. Reimer, Y. Sanjiev, and the HERMES Collaboration)

HERMES, HERA Measurement of Spin, is a second-generation experiment to study the spin structure of the nucleon by using polarized internal gas targets in the HERA 30 GeV electron storage ring. Since 1995, the experiment has provided fundamental new insights into the structure of the nucleon and how it is affected by the nuclear medium. The unique capabilities of the experiment have produced data that were not possible with previous measurements at SLAC, CERN, and Fermilab. The collaboration has collected and analyzed millions of deep-inelastic scattering events using longitudinally polarized electrons and positrons incident on longitudinally polarized internal gas targets of ^1H , ^2H , and ^3He , as well as thicker unpolarized gas targets. These data together with large sets of photo-production events have yielded several results that were unexpected and are provoking new work, both theoretical and experimental.

The primary goal of HERMES is the study of the spin structure of the nucleon. Spin asymmetries have been measured using polarized targets of hydrogen, deuterium, and ^3He . Analysis of the inclusive and

semi-inclusive deep-inelastic scattering data from these unique undiluted targets has resulted in the world's most precise determination to date of the separate contributions of the up, down and sea quarks to the nucleon spin.¹ Further dramatic improvements are expected from the data under analysis. One of the surprises yielded by the experiment was a negative polarization asymmetry (though with large statistical uncertainty) in the cross section for photo-production of pairs of hadrons with high transverse momenta, providing the first direct indication of a positive gluon spin contribution to the nucleon. Again, recent and future data will much improve the statistical precision. Another exciting result is the observation of a single-spin asymmetry in the azimuthal distribution of positive pions detected in coincidence with the deep-inelastic scattering of positrons from a *longitudinally* polarized proton target. While the theoretical interpretation of this result is under vigorous discussion, it seems clear that the effect can be explained only by a particular chiral-odd fragmentation function that promises to make feasible at HERMES the first measurement of transversity, the only remaining unmeasured and one of

the three most fundamental (leading twist) flavor-sets of parton distribution functions. Finally, a result from HERMES of great interest has been the first measurement of a lepton-beam spin asymmetry in the azimuthal distribution of detected photons in Deeply Virtual Compton Scattering (DVCS). Interference with the indistinguishable but well-understood Bethe-Heitler process fortuitously gives rise to a rich variety of such asymmetries, which will continue to emerge from HERMES data. DVCS is considered to be the most reliable of the various hard exclusive processes that constrain the generalized or 'skewed' parton distributions, which are now the subject of intense theoretical development as, *e.g.*, they embody information about *orbital* angular momenta of partons. Most recently, this type of measurement has been extended to the study of exclusive electroproduction of pions, where substantial single-spin azimuthal asymmetries have been observed for the first time.

The HERMES physics reach extends well beyond nucleon spin structure. The large momentum and solid angle acceptance of the HERMES spectrometer have opened a much broader range of physics topics to exploration, and have resulted in a tool for the general study of photon-hadron interactions. Focusing its unique capabilities on specific applications of deep-inelastic scattering (DIS), HERMES has performed a measurement of the flavor asymmetry between up and down quarks in the nucleon sea,² several studies of fragmentation of up and down quarks to pions, measurement of the DIS and resonance contributions to the generalized Gerasimov-Drell-Hearn integral for both the proton and neutron,^{3,4} a measurement of the spin transfer from virtual photons to Λ^0 hyperons,⁵ and measurements of the effect of the nuclear environment. A broad program of measurements involving diffractive vector meson production is also underway with basic studies in ρ^0 , ϕ^0 , ω^0 , and J/ψ production,⁶ as well as the determination of photon \rightarrow vector-meson spin density matrix elements through the analysis of the angular distribution of the decay products.⁷ The ρ^0 semi-exclusive cross section has been found to have a large and unexpected spin dependence.⁸ The study of diffractive ρ^0 production in nuclei has led to the

observation of a lifetime (coherence length) effect on the initial-state nuclear interactions of the virtual quark pair that represent the hadronic structure of the photon, and will lead to new limits on the magnitude of color transparency effect.⁹ Recent developments and new results pertaining to these physics topics are discussed in more detail below, and references may be found at the end of this report. It is evident that HERMES has a broad physics program and has had scientific impact on an impressive number of fundamental questions about the strong interaction. HERMES is playing an important role in the worldwide experimental investigation of QCD.

The experiment is technically sound. The means to produce and measure high beam polarization and high target polarization are well understood. The spectrometer and its instrumentation have been carefully modeled and operate reliably and in an understandable fashion. Data analysis software and computational power are now at an advanced stage, allowing the collaboration to produce results in a timely fashion. Furthermore, a vigorous upgrade program has continued to enhance the capabilities of the spectrometer. The gas threshold Cerenkov detector was replaced by a dual-radiator ring-imaging Cerenkov (RICH) detector to identify pions, kaons, and protons over nearly the entire momentum acceptance, and both a new iron wall and the iron of the spectrometer magnet were instrumented to improve the acceptance and identification of high energy muons from charm decay. Finally, preparations are being made for the installation in the first months of 2002 of two new rings of silicon strip detectors just downstream of the target, primarily to enhance the detection of Λ^0 decay products. As will be discussed below, the combination of all these new detectors opens the door to new exciting measurements. This extraordinary and unique facility represents the investment of nearly a thousand person-years and 40 MDM, from over 33 institutes from 10 countries in Europe, Asia and North America. Nevertheless, in comparison with other experiments and laboratories, it is highly cost-effective with respect to its productivity and potential.

¹K. Ackerstaff *et al.*, Phys. Lett. B **464**, 123 (1999)

²K. Ackerstaff *et al.*, Phys. Rev. Lett. **81**, 5519 (1998)

³K. Ackerstaff *et al.*, Phys. Lett. B **444**, 531 (1998)

⁴A. Airapetian *et al.*, DESY 00-097, hep-ex/0008037

⁵A. Airapetian *et al.*, DESY 99-151, hep-ex/9911017

⁶A. Airapetian *et al.*, accepted by Eur. Phys. J.C

⁷K. Ackerstaff *et al.*, DESY 99-199, hep-ex/0002016

⁸F. Meissner, Proceedings of the 7th International Workshop on Deep Inelastic Scattering and QCD, Zeuthen, Germany, April 1999

⁹K. Ackerstaff *et al.*, Phys. Rev. Lett. **82**, 3025 (1999)

c.3. Inclusive Measurements of the Deuteron Spin structure Function (H. E. Jackson, A. El Alaoui, K. G. Bailey, T. P. O'Connor, K. Hafidi, D. H. Potterveld, P. Reimer, Y. Sanjiev, and the HERMES Collaboration)

Inclusive measurements of the spin structure functions for the proton and neutron continue to be an important element in the HERMES program. Measurements of $g_1^d(x)$ provide the basic data for the neutron structure function. The inclusive deuteron spin asymmetries are also an essential component of the global analysis of spin asymmetries used in the flavor decomposition of the polarized quark structure functions of the nucleon. HERMES has precisely determined the spin structure functions of both the proton and neutron, $g_1^p(x)$ and $g_1^n(x)$, over a range in Bjorken x from approximately ~ 0.001 to ~ 0.8 , using various beams, targets and spectrometers.

Results of the measurement of the inclusive spin dependent asymmetry from HERMES, and CERN/SMC are shown in Fig. IV-11, where the ratio g_1^d/F_1 of the deuteron is plotted. The data sets are in remarkable agreement, thus demonstrating that the experimental uncertainties are well understood. As the SMC data have an average Q^2 that is about a factor of 3 to 10 larger than those of the SLAC and the HERMES measurements, the Q^2 dependence of the asymmetry g_1/F_1 is revealed to be small. Such data have strongly confirmed the earlier EMC result and extended the range and precision of the knowledge of g_1 , which provides a strong constraint for all models and parameterizations of the polarized quark distributions.

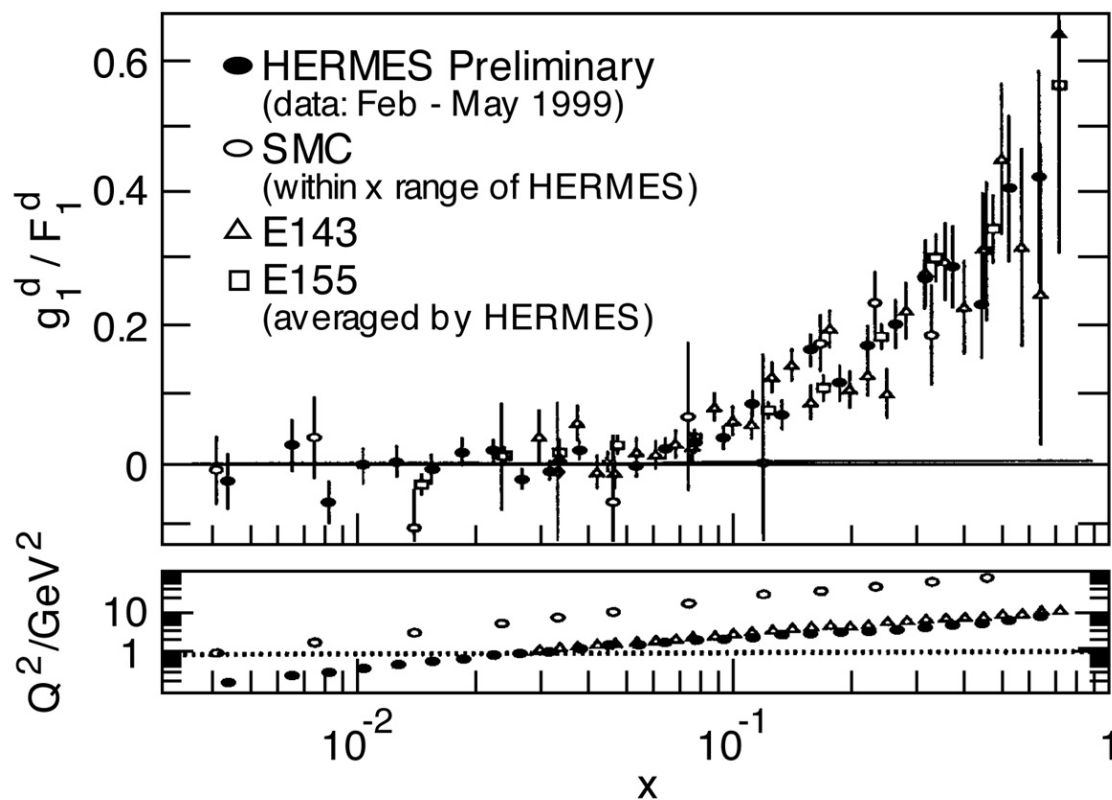


Fig. IV-11. The HERMES measurement of g_1^d compared to SLAC-143 and CERN/SMC. All data are given at their quoted mean Q^2 .

c.4. Flavor Decomposition of Polarized Structure Functions (H. E. Jackson, A. El Alaoui, K. G. Bailey, T. P. O'Connor, K. Hafidi, D. H. Potterveld, P. Reimer, Y. Sanjiev, and the HERMES Collaboration)

Information from inclusive scattering is inherently limited by the domination of scattering from up quarks, since the cross sections scale as the square of the electric charge, which is twice as large for up quarks as for down or strange quarks. Also, quarks and antiquarks of the same flavor obviously produce identical effects. To distinguish the contributions of the quark flavors and in particular of the sea quarks, it is necessary to use other types of experimental information. In semi-inclusive scattering, a leading hadron is detected in coincidence with the deep-inelastic scattering of a lepton. The essential principle behind this method is the likelihood of the leading hadron to 'contain' the quark originally struck by the virtual photon from the lepton. Scattering asymmetries with various leading hadrons in the final state can be analyzed to determine the fractional contributions of the various quark flavors to the nucleon spin.

The HERMES collaboration is in the process of determining the flavor dependence of quark polarizations in the nucleon in a global analysis of inclusive and semi-inclusive spin asymmetries for positive and negative pions and kaons which assumes a five component decomposition of quark spin, *i.e.* u, \bar{u}, d, \bar{d} , and $s + \bar{s}$. Data are included for both proton and deuteron targets. Factorization into parton distributions and fragmentation functions is assumed in the relation between the measured asymmetries and quark polarizations. The resulting coefficients or "purities" include effects of experimental acceptance, and are determined with a Monte Carlo generator and CTEQ low Q^2 parton distributions. An independent two-component purity analysis using only the deuteron inclusive and total kaon semi-inclusive asymmetries provides an independent check on the results for the polarization of the strange sea. The first complete analysis is in its final stages, and results will be released in the spring of 2002.

c.5. Gluon Polarization (H. E. Jackson, A. El Alaoui, K. G. Bailey, T. P. O'Connor, K. Hafidi, D. H. Potterveld, P. Reimer, Y. Sanjiev, and the HERMES Collaboration)

A measurement of the polarization of the gluons in the nucleon is of central importance to understanding the origin of the spin of the nucleon. A promising prospect is a direct measurement of $\Delta G(x)$ using scattering processes in which the gluon enters in leading order. Such a lepto-production process is photon-gluon fusion (PGF). Experimental signatures of this process are charm production and the production of jets on hadrons with high transverse momentum. Both of these signals have been successfully exploited at higher energy in measurements of the unpolarized gluon structure function. Such measurements are central goals of the COMPASS experiment¹ at CERN and of the RHIC-SPIN groups in the experiments STAR and PHENIX.² At HERMES the spin asymmetry in the polarized photo-production of pairs of hadrons with opposite charge and high transverse momentum has been studied.³ Under certain kinematical conditions, this signal is dominated by PGF, which has a strong negative polarization analyzing power.

A published HERMES result for the highest transverse momenta accessible suggested that gluons have a significant positive polarization. For h^+h^- pairs with $p_T^{h_1} > 1.5$ GeV/c and $p_T^{h_2} > 1.0$ GeV/c, the spin asymmetry is found to be $A_{||} = -0.28 \pm 0.12$ (stat) ± 0.02 (sys). This negative value is in contrast to the positive asymmetries typically measured in deep-inelastic scattering from protons. When these data are interpreted in a LO QCD model implemented in the PYTHIA Monte Carlo generator, a value for $\Delta G(x)/G(x)$ of $0.41 \pm 0.18 \pm 0.03$ has been determined at $\langle x_G \rangle = 0.17$. The sensitivity of the HERMES measurement can be increased by using high- p_T kaon pairs. The production of strange hadrons in fragmentation is suppressed compared to non-strange hadrons, with the result that background from DIS will be suppressed, and the sample of kaon pairs will be cleaner than the corresponding pion sample. For this reason, in the HERMES analysis, a lower cut on $p_T^{h_1}$ could be used to improve statistics. Fig. IV-12 shows preliminary results for high- p_T kaon pairs from proton and deuteron targets. The data are still under study, and

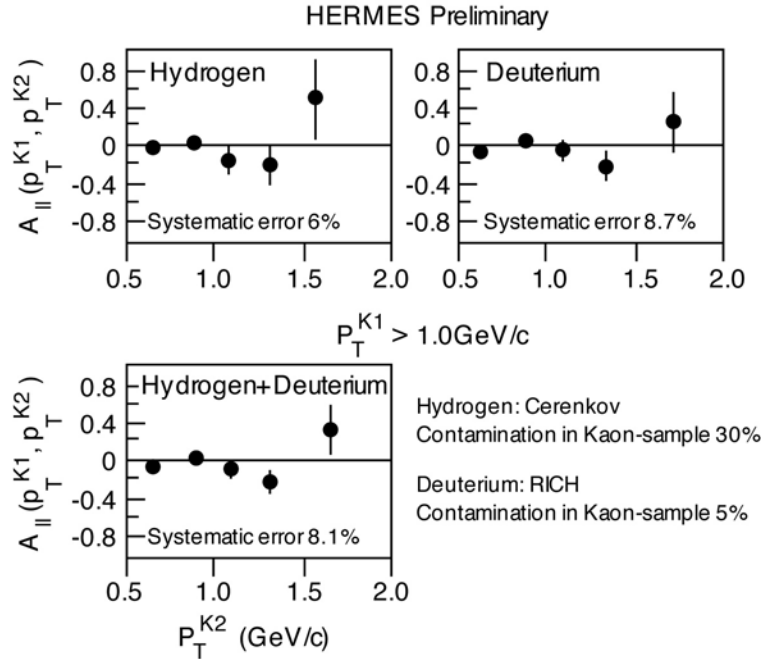


Fig. IV-12. The HERMES measurement of the double-spin asymmetry $A_{||}(p_T^{k+}, p_T^{k-})$ for polarized proton and deuterium targets. The error bars represent statistical errors.

the Monte Carlo treatment of the analyzing powers using the PYTHIA event generator is being refined. Nevertheless, the asymmetries observed for kaons

appear to be consistent with earlier conclusions of a positive gluon polarization.

¹The COMPASS Collaboration, CERN/SPSLC 96-14 (1996)

²PHENIX, BNL-PROPOSAL-R5, Aug. 1992; STAR, S. E. Vigdor *et al.*, hep-ex/9905034

³A. Airapetian *et al.*, Phys. Rev. Lett. **84**, 2584 (2000)

c.6. Azimuthal Asymmetries and Transversity (H. E. Jackson, A. El Alaoui, K. G. Bailey, T. P. O'Connor, K. Hafidi, D. H. Potterveld, P. Reimer, Y. Sanjiev, and the HERMES Collaboration)

Using a longitudinally polarized target, HERMES has recently reported the first observation of a single-spin asymmetry in the azimuthal distribution of hadrons detected in coincidence with deep-inelastic lepton scattering. The sinusoidal target-related spin asymmetry corresponds to an analyzing power of 0.022 ± 0.005 (stat) ± 0.003 (sys) for positive pions, and is consistent with zero for negative pions. It has been found¹ that these data are consistent with models for the relevant distribution functions together with a model for the Collins fragmentation function that is also consistent with a preliminary value for this function from $Z^0 \rightarrow 2\text{-jet}$ decay.² Hence it appears that the Collins fragmentation function is responsible for the

effect and has a substantial value, thus opening the way to future measurements of transversity using transversely polarized targets. Transversity h_1 is the third of three structure functions required to describe the structure of the nucleon in leading order. It is of fundamental interest because it is an all valence object which does not couple to gluons, and consequently, is expected to have unique scaling properties.

Recently these results have been extended³ to neutral pions. As with charged pions, a distinct $\sin\phi$ dependence is observed in the pion production asymmetry $A_{UL}(\phi)$ with respect to longitudinal target polarization. Here ϕ is the azimuthal angle of the pions

relative to the lepton scattering plane, around the virtual photon direction. In Fig. IV-13 the $\sin(\phi)$ moment of the asymmetry ($A_{UL}^{\sin\phi}$) is shown as a function of the pion fractional energy z , the Bjorken scaling variable x and the pion transverse momentum P_{\perp} . The π^0 and π^+ asymmetries exhibit a similar behavior in all kinematic variables, while the π^- asymmetry is consistent with zero. This is consistent with the expected dominance of scattering from u-quarks in the first two cases. The increase of the asymmetries with x suggests that they are associated with valence quark contributions. The

dependence on P_T may be related to the dominant kinematic role of intrinsic quark transverse momentum in the region where P_{\perp} remains below the typical hadronic mass scale of ≈ 1 GeV. The results have been successfully interpreted in terms of the unknown transversity function $h_1(x)$ together with the chiral-odd Collins fragmentation function $H_1^{\perp}(z)$. New data will be forthcoming from future HERMES measurements on a transversely polarized target, which will give direct access to transversity.

¹A. M. Kotzinian *et al.*, hep-ph/9908466

²A. V. Efremov, O. G. Smirnova, and L. G. Tkachev, Nucl. Phys. Proc. Suppl. **74**, 49 (1999)

³A. Airapetian *et al.*, Phys. Rev. Lett. **84**, 4047 (2000)

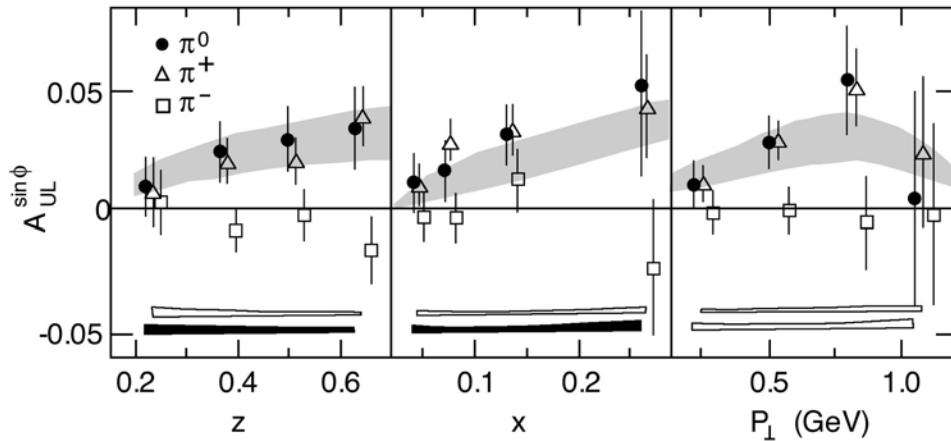


Fig. IV-13. The $\sin\phi$ moment of the asymmetry A_{UL} for π^0 production compared to previous HERMES results for π^+ and π^- . The open and filled bands represent the systematic uncertainties for neutral and charged pions respectively. The data for charged pions are shifted slightly for clarity.

c.7. Measurements With Unpolarized Targets: Hadron Formation Times (H. E. Jackson, A. El Alaoui, K. G. Bailey, T. P. O'Connor, K. Hafidi, D. H. Potterveld, P. Reimer, Y. Sanjiev, and the HERMES Collaboration)

HERMES has an active program of measurements with unpolarized targets which addresses a range of topics in photon-hadron interactions. As an example, HERMES has measured the charged pion fragmentation functions for up and down quarks from the nucleon, and their attenuation in a nuclear environment. By embedding the fragmentation process in the nuclear medium, one can study the time propagation of the hadron formation process. The attenuation of hadrons, which is measured as a function of the energy transfer ν and the hadron energy fraction $z = E_h/\nu$, can be related to the formation length (or time) of the hadron, or can be compared directly to model calculations. In fact, such data can also be used to derive empirical values for the hadron formation time and the energy loss of a quark

propagating in the medium. These quantities are of considerable theoretical and experimental interest, as it is possible to apply the same concepts in the description of the Drell-Yan process and heavy-ion collisions.

HERMES has recently released data on the attenuation ratios for nitrogen and krypton which have provoked widespread interest. The experimental results are developed as a multiplicity ratio which represents the ratio of the number of hadrons produced per DIS event for a nuclear target to that from a deuterium target. These data have been interpreted¹ in terms of final state interactions which soften the quark fragmentation functions. This medium modification of the fragmentation of the propagating parton results from

induced gluon radiation due to multiple parton scattering, and gives rise to additional terms in the QCD evolution equations that soften the fragmentation functions. As shown in Fig. IV-14, this treatment provides an excellent description of the HERMES

results. From these data, this treatment gives a quark energy loss of $dE/dx \approx 0.5$ GeV/fm in cold nuclear matter.

¹E. Wang, X.-N. Wang, LBNL-4956 (Feb 2002), hep-ph/0202105

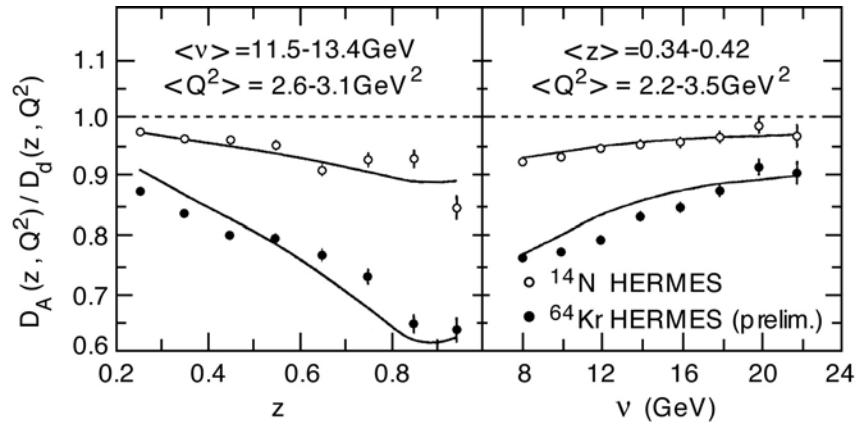


Fig. IV-14. At left, predicted nuclear modification of jet fragmentation functions (curves) compared to HERMES data on the ratios of hadron distributions between A and D targets in DIS. At right, the energy dependence of this predicted nuclear modification (curves) compared to the HERMES data.

c.8. A Dual Radiator Ring Imaging Cerenkov Counter for HERMES (H. E. Jackson, A. El Alaoui, K. G. Bailey, T. P. O'Connor, K. Hafidi, D. H. Potterveld, P. Reimer and the HERMES Collaboration)

A dual radiator Ring Imaging Cerenkov (RICH) detector for the identification of hadrons¹ has been in operation as part of the HERMES spectrometer since 1998. The HERMES experiment emphasizes measurements of semi-inclusive deep-inelastic scattering. However, most of the hadrons produced lie between 2 and 10 GeV, a region in which it had not previously been feasible to separate pions, kaons, and protons with standard particle identification (PID) techniques. The recent development of new clear, large, homogeneous and hydrophobic silica aerogel material with a low index of refraction offered the means to apply RICH PID techniques to this difficult momentum region for the first time. The HERMES instrument uses two radiators, C₄F₁₀, a heavy fluorocarbon gas, and a wall of silica aerogel tiles. A lightweight spherical mirror constructed using a newly perfected technique to make resin-coated carbon-fiber surfaces of optical quality provides optical focusing on a photon detector consisting of 1934 photomultiplier tubes (PMT) for each detector half. The PMT array is held in a soft steel matrix to provide shielding against the residual field of the main spectrometer magnet.

Ring reconstruction is accomplished with pattern recognition techniques based on a combination of inverse and direct ray tracing.

The Argonne group led the design and construction of the HERMES RICH, an effort which involved 8 collaborating institutions. With the successful commissioning of the system, attention turned to debugging, testing, and implementing the software required for data analysis. The identification of the different hadrons in the HERMES RICH detector is based on two different methods: the indirect ray tracing method (IRT) and the direct ray tracing method (DRT). Both methods are combined in a likelihood analysis which selects the most probable particle type. The IRT and DRT method exist in parallel; a decision network chooses the optimal method depending on the event topology. To date, as shown in Fig. IV-15, the IRT method has been demonstrated to give reliable results. Work continues on testing and tuning the DRT method. With the demonstration of reliable operation of the DRT method, a final training of the decision network will be performed, in order to implement its use in

providing the highest efficiency for reliable particle identification (PID). The efficiencies for particle identification are measured experimentally by using decaying ϕ , K_s , and Λ particles. Because of the limited topologies of this class of events, it is necessary to use a

Monte Carlo simulation to extend these efficiencies to a more extensive range of topologies. Work in this area continues. A careful analysis of error propagation in PID efficiencies remains to be done.

¹N. Akopov *et al.*, Nucl. Instr. Meth. A **479**, 511 (2002)

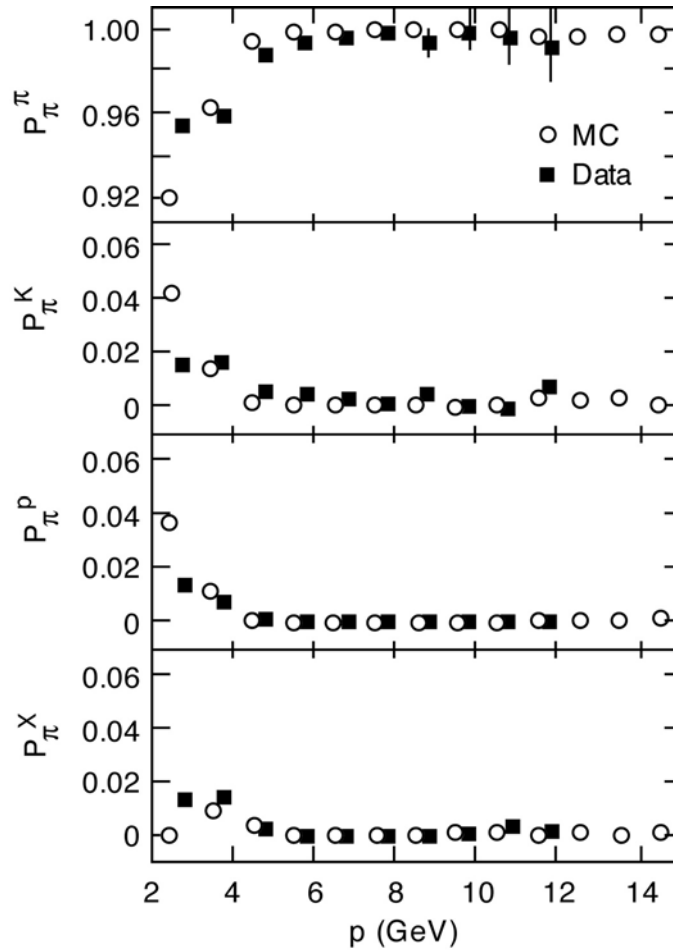


Fig. IV-15. Identification probabilities P_{π}^i that a pion is identified as pion, kaon, proton, or not identified (X) for single tracks per detector half. MC simulations (circles) in comparison with experimental data from ρ_0 - decays (solid squares); both results are based on the IRT likelihood analysis.

c.9. Nuclear Dependence of Lepton Pair Production: Parton Energy Loss, Shadowing and J/ψ and ψ' Suppression (D. F. Geesaman, S. B. Kaufman, N. C. R. Makins, B. A. Mueller, P. E. Reimer and the FNAL E866/NuSea Collaboration)

Through comparisons of production cross sections from different nuclear targets, we can deduce information about the behavior of quarks in a strongly interacting environment and learn how nuclear size affects the interaction processes. FNAL E866/NuSea collected Drell-Yan, J/ψ , and ψ' production data using Beryllium, Iron and Tungsten targets.

In the Drell-Yan process, the colored initial-state quarks (and antiquarks) from the beam interact strongly as they pass through the target nucleus before annihilating into a virtual photon. After the annihilation, the final state muons do not have significant interactions with the nuclear medium. In these strong initial state interactions, the quarks should lose some of their energy. Using the ratios of Drell-Yan cross sections from a variety of nuclear targets, and comparing with different models for the energy, tight limits were placed on the energy loss of a parton traveling through cold nuclear matter.

Before making these comparisons, it was necessary to account for a phenomenon known as shadowing, which manifests itself as a depletion in quark density at low x_{target} (the fractional momentum of carried by the struck

quark in the target) in heavy nuclei relative to light nuclei. Although not completely understood, it is well parameterized from Deep Inelastic Scattering (DIS) data. By comparing the Drell-Yan yields from nuclear targets we were able to confirm that shadowing in Drell-Yan quantitatively matches predictions based on shadowing in DIS. Since the observed Drell-Yan shadowing agrees with the DIS parameterizations, it was possible to remove this nuclear dependence from the quark energy loss analysis, described above.

Another nuclear effect, known as “suppression” causes the rate of production of J/ψ , and ψ' mesons in proton nucleus collisions to be diminished relative to the same process with a proton target. While the above-mentioned shadowing certainly plays an important role in this suppression, it is not the entire explanation. Using nuclear targets, E866/NuSea studied suppression as a function of the kinematic variables, Feynman- x (x_F) and transverse momentum (p_t). At low values of x_F , the surprising observation was made that the ψ' is more suppressed than the J/ψ , an effect that may be attributable to the absorption of the $c\bar{c}$ pair in the nucleus before hadronization.

c.10. Production of Υ and J/ψ from 800 GeV Protons Incident on Hydrogen and Deuterium (D. F. Geesaman, S. B. Kaufman, N. C. R. Makins, B. A. Mueller, P. E. Reimer and the FNAL E866/NuSea Collaboration)

Υ and J/ψ mesons are produced when partons from the beam and target annihilate and form a virtual gluon, which then hadronizes into a heavy meson resonance. The virtual gluon that produced the resonance can be generated by the annihilation of either a quark-antiquark pair or a pair of gluons (also called gluon-gluon fusion). Hence resonance production is sensitive to both the quark and gluon distributions with the target and beam. The J/ψ is believed to be produced primarily through gluon-gluon fusion, while Υ production is thought to proceed via both gluon-gluon fusion and quark-antiquark annihilation. Because the gluon distribution for the proton and neutron are similar, the per nucleon J/ψ cross section should be the same for both hydrogen and deuterium. For the Υ , on the other hand, the ratio of deuterium to hydrogen cross sections is expected to be larger than unity for the values of fractional momenta, x , probed by FNAL E866/NuSea,

since $\bar{u}_n > \bar{u}_p$, in this region, which allows for more $u_{\text{beam}} - \bar{u}_{\text{target}}$ annihilations with deuterium.

The FNAL E866/NuSea hydrogen and deuterium data contain 30 thousand Υ and one million J/ψ events. The production cross sections for these mesons have been extracted and can be compared to predictions based on models and parton distributions available in the literature. Color evaporation model calculations have been performed for both Υ and J/ψ production from hydrogen and deuterium. Although it is an extremely simple model and cannot predict the absolute value of the cross section, the color evaporation model does reproduce the observed x -Feynman shape of the cross section. In addition, when looking at the ratio of deuterium to hydrogen per nucleon cross sections, the unknown scale factor drops out. The measured cross

section ratios for both the J/ψ and the Υ are near unity as shown in Fig. IV-16. In the case of the J/ψ , this is not surprising, since J/ψ production is expected to proceed through gluon fusion. In the case of the Υ , however, the value near unity is in disagreement with color evaporation model calculations. The color

evaporation model also fails to explain the large transverse polarization seen in Υ production as discussed in the next section. This deviation may indicate that the parton distribution functions underestimate the hard gluon ($x \approx 0.25$) distribution in the proton.

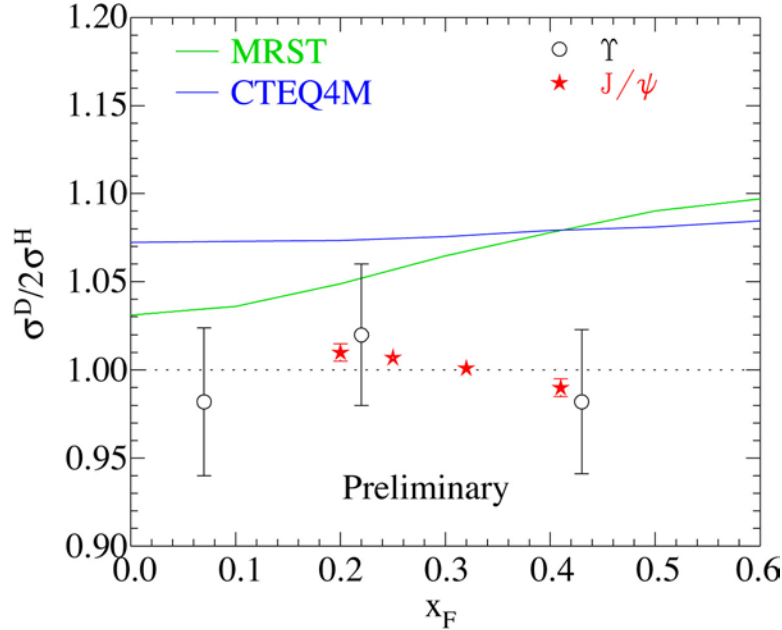


Fig. IV-16. The data points show the ratio of cross section for J/ψ and Υ production from deuterium to hydrogen. The curves represent color evaporation model calculations for this ratio for Υ production using two different parameterizations of the nucleon parton distributions. (J/ψ production is expected to have a ratio near unity.)

c.11. Polarization Measurement of Υ and ψ Production in Proton-Nucleus Collisions (D. F. Geesaman, S. B. Kaufman, N. C. R. Makins, B. A. Mueller, P. E. Reimer, and FNAL E866/NuSea Collaboration)

Despite Quantum Chromodynamics' (QCD) overwhelming success in describing many aspects of the strong interaction, an adequate description of quarkonia production is still lacking, due, in part, to its non-perturbative nature. Various models of quarkonia production have been proposed, including Color Octet and Color Singlet models. These models make definite predictions for the polarization of the produced quarkonia. Due to the clean experimental signature provided by their di-lepton decay mode, the Υ and ψ meson families provide important systems in which to study this. FNAL E866/NuSea has measured the polarization of the Υ and ψ mesons produced in proton-nucleus collisions.

In data from FNAL E866/NuSea, the $\Upsilon(1S)$ is seen to exhibit only slight polarization, and that only at large x -

Feynman (x_F) or large transverse momenta (p_T). Unfortunately, the $\Upsilon(1S)$ resonance is not the ideal place in which to study hadronization, since the observed $\Upsilon(1S)$ signal contains not only directly produced Υ 's but also Υ 's produced indirectly through the decay of higher mass $b\bar{b}$ states. Thus, the signal is less sensitive to the $b\bar{b}$ production mechanism. Due to their higher mass, the $\Upsilon(2S)$ and $\Upsilon(3S)$ have fewer states which can feed their production and the observed polarization better reflects the inherent production mechanism. FNAL E866/NuSea observes nearly complete transverse polarization in these two states (unresolved) as shown in Fig IV-17. Color octet production, but not color evaporation models are consistent with the present results.

In the ψ family, the J/ψ is observed to have only a slight polarization which changes from transverse to longitudinal as a function of x_F . Once again, however, the polarization signal from direct production is diluted

by feed down from other $c\bar{c}$ states. Data on the polarization of the ψ' is currently under analysis. While statistics are limited, this state has the advantage that the entire signal is from direct production.

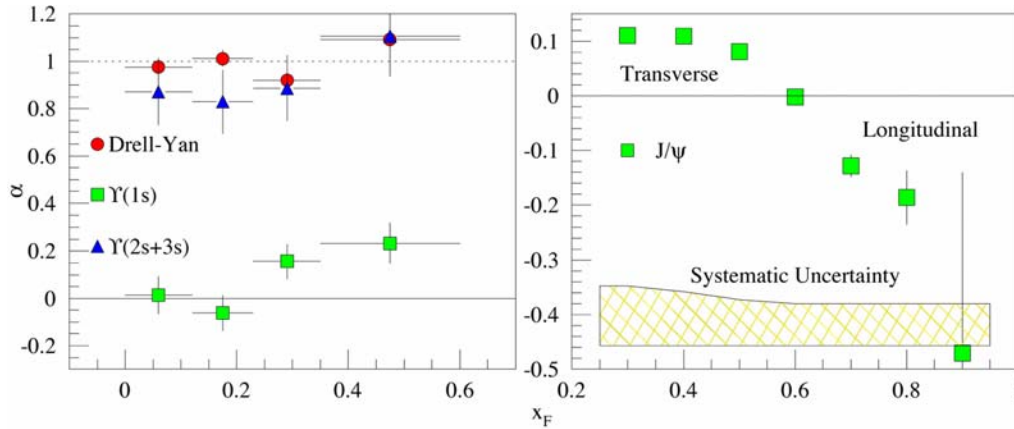


Fig. IV-17. The observed polarization of the $Y(1S)$ and the unresolved $Y(2S,3S)$ (left) as a function of Feynman- x , x_F . The observed polarization of the J/ψ (right) as a function of x_F .

c.12. Measurement of the Antiquark Flavor Asymmetry of the Proton Sea Using Drell-Yan Scattering (D. F. Geesaman, S. B. Kaufman, N. C. R. Makins, B. A. Mueller, P. E. Reimer, and FNAL E866/NuSea Collaboration)

While it is not required by any fundamental symmetry, it has—until recently—been widely assumed that the distributions of anti-down, \bar{d} , and anti-up, \bar{u} , quarks in the proton were identical. This was based on the assumption that the proton's sea arose perturbatively from gluons splitting into quark-antiquark pairs. Since the mass difference between the up and down quarks is small, equal numbers of up and down pairs would result. A ratio of \bar{d}/\bar{u} which is not unity is a clear sign of nonperturbative origins to the quark-antiquark sea of the proton, and recent evidence from deep inelastic scattering has shown an integral difference between the anti-up and anti-down distributions.

To further explore this difference, Fermilab E866/NuSea measured the ratio \bar{d}/\bar{u} as a function of the momentum carried by the struck quark, x . This was accomplished using the Drell-Yan mechanism, in which, a quark (or antiquark) in the proton beam annihilates with an antiquark (or quark) in the target. The resulting annihilation produces a virtual photon that decays into a pair of leptons, which are seen in the detector. Data were collected in 1996-1997 with the Meson East Spectrometer at Fermilab using an 800 GeV/c proton beam on hydrogen and deuterium targets.

From the ratio of hydrogen to deuterium Drell-Yan cross sections, the ratio \bar{d}/\bar{u} and difference $\bar{d}-\bar{u}$ have been extracted, and unexpected x -dependent flavor asymmetry in the proton's sea was revealed. The flavor difference in pure flavor non-singlet: Its integral is Q^2 independent and its Q^2 evolution, at leading order, does not depend on the gluon distributions in the proton. The large differences seen in Fig. IV-18 must be non-perturbative in nature. Several approaches have been suggested which could produce this difference. They include meson cloud models of the nucleon,¹ chiral quark models in which the mesons couple directly to the constituent quarks² chiral soliton and instanton models.³ These models are illustrated by the curves in Fig. IV-18.

The Drell-Yan absolute cross sections are also being extracted from the hydrogen and deuterium data. While the ratio of Drell-Yan cross sections is sensitive to the relative strength of the different flavors of anti-quarks, the absolute cross sections are sensitive to the total strength of the anti-quark sea, \bar{d}/\bar{u} . The Drell-Yan cross section is easily calculable next-to-leading order in α_s and can be compared directly with the measured

cross sections. Measurements were also made of the nuclear dependence of J/ψ , ψ' and Drell-Yan

production using Be, Fe, and W targets and of the polarization of the J/ψ , ψ' and Υ states.

¹J. C. Peng *et al.* (FNAL E866/NuSea Collaboration, Phys. Rev. D **58**, 092004 (1998); N. Nikoleav *et al.* Phys. Rev. D **60**, 014004 (1999)

²A. Szczurek *et al.* J. Phys. G **22**, 1741 (1996); P. V. Pobylitsa *et al.* Phys. Rev. D **59**, 034024 (1999)

³A. E. Dorokhov and N. I. Kochelev, Phys. Lett. B, 335 (1991); Phys. Lett. B **304** 167 (1993)

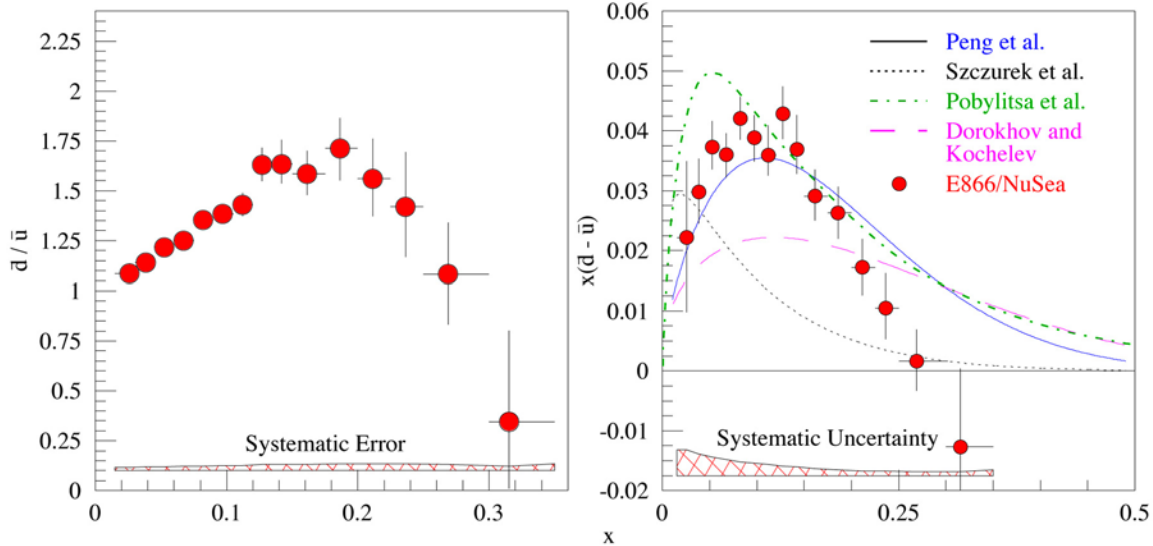


Fig. IV-18. The ratio of \bar{d}/\bar{u} (left) and $x(\bar{d}/\bar{u})$ (right) as a function of x , the fraction of the proton's momenta carried by the struck quark. The curves in the right graph represent different model calculations as described in the text.

c.13. Drell-Yan Measurements with 120 GeV Protons, FNAL E906 (D. F. Geesaman, K. Hafidi, R. J. Holt, D. H. Potterveld, P. E. Reimer, and the FNAL E906 Collaboration)

The Drell-Yan measurements of Fermilab E866/NuSea have provided new insight into the antiquark sea in the proton and nuclear dependence phenomena. FNAL E906 has been approved by Fermilab to extend Drell-Yan measurements to larger values of x (the fraction of the proton's momenta carried by the struck quark) using the new 120 GeV Main Injector at Fermilab.

FNAL E866/NuSea's measurements of ratio of anti-down, \bar{d} , to anti-up, \bar{u} , quarks in the proton, \bar{d}/\bar{u} , revealed an unexpected x -dependence. At small x this ratio increases from unity to a maximum asymmetry of over well 50%, as expected. For $x \geq 0.19$, however, the ratio of \bar{d}/\bar{u} decreases and becomes symmetric again at the highest values of x accessible to the experiment.¹ Unfortunately, in this region, the statistical uncertainty of the data also becomes large. E906 will be able to significantly reduce the statistical uncertainty of the data and extend these measurements to even larger

values of x . The expected sensitivity of E906 to the \bar{d}/\bar{u} ratio is shown in Fig. IV-19. In this higher- x region, E906 will be sensitive to the interplay between the nonperturbative and the perturbatively generated sea.

In addition to hydrogen and deuterium targets, the experiment will collect data with a number of heavy nuclear targets. These data will allow a systematic study of nuclear effects in the Drell-Yan process. Since the Drell-Yan process is sensitive to antiquark distributions, any enhancement in the sea due to nuclear effects (virtual pion contributions to nuclear structure functions) should be apparent in the ratio of Drell-Yan cross sections from nuclear targets. Previous data² from FNAL E772, however, did not show these enhancements. FNAL E906 will significantly reduce this statistical uncertainty and extend these measurements to larger x , where the effect is expected

to be greater. Additionally, the absolute magnitude of the proton's sea high- x distributions are derived from neutrino-nucleus deep inelastic scattering (DIS) data and may have unknown nuclear effects. By comparing light and heavy target Drell-Yan data, the experiment will be making a measurement of these effects. A comparison with muon-induced DIS will provide the ability to differentiate between valence and sea-based nuclear effects. The expected statistical uncertainty of E906 nuclear data and existing Drell-Yan and muon DIS are shown in Fig. IV-19.

Using the same nuclear target data, the energy loss of colored partons traveling through a strongly interacting media will be studied. E906's predecessor, FNAL E866/NuSea was able to extract upper limits on this energy loss within the context of several models.³ At the lower energy of the Main Injector, the energy loss is expected to be much greater, and the new data will be able to distinguish between these and other models.⁴ These measurements are important for RHIC where jet

quenching is expected to be an important signal for the formation of a Quark-Gluon Plasma.

FNAL E906 is able to make these improvements over previous measurements because of the lower beam energy available at the Fermilab Main Injector. For fixed x_1 and x_2 the cross section scales as the inverse of the beam energy. Thus a factor of seven more events for the same integrated luminosity can be achieved. At the same time, the primary background to the measurement, muons from J/ψ decays, decreases with increasing beam energy, allowing for an increase in instantaneous luminosity by another factor of seven. These two factors combine to provide roughly 50 times more events for the same beam time.

FNAL E906 has been approved by the Fermilab PAC and will most likely begin collecting data in late 2007. In the mean time, a number of new detector elements must be constructed, the most significant of which is a new large dipole magnet to focus the Drell-Yan muons.

¹E. A. Hawker *et al.* (FNAL E866/NuSea collaboration), Phys. Rev. Lett. **80**, 3715 (1998); R. S. Towell *et al.* (FNAL E866/NuSea Collaboration), Phys. Rev. D **64**, 052002 (2001)

²D. M. Alde *et al.* (FNAL E772 Collaboration), Phys. Rev. Lett. **64**, 2479 (1990)

³M. A. Vasiliev *et al.* (FNAL E866/NuSea Collaboration), Phys. Rev. Lett. **83**, 2304 (1999)

⁴M. B. Johnson *et al.* Phys. Rev. C **65**, 025203 (2002); M. B. Johnson *et al.* (FNAL E772 Collaboration) Phys. Rev. Lett. **86**, 4483 (2001)

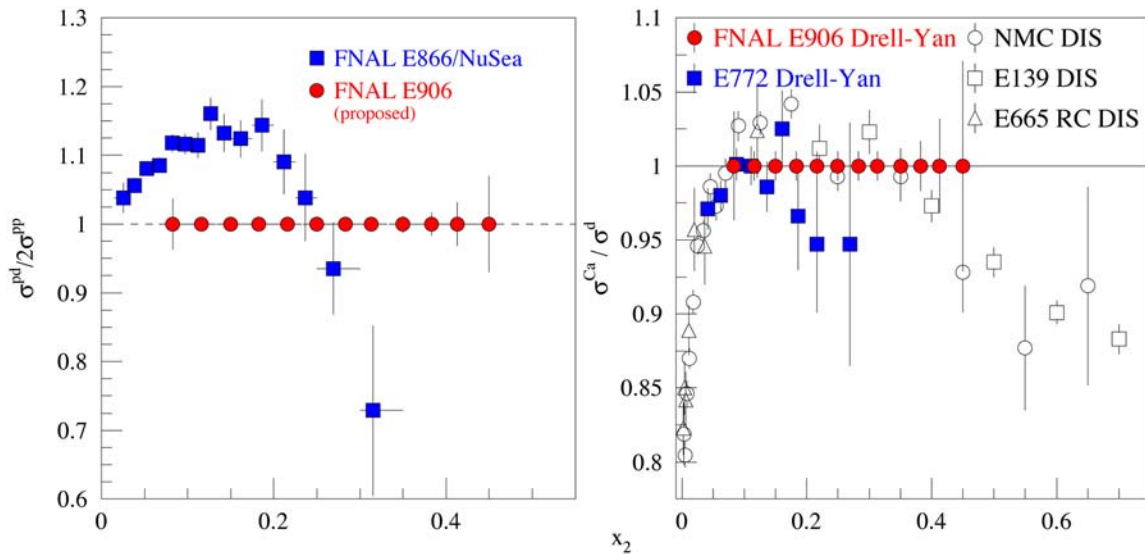


Fig. IV-19. The statistical uncertainty of E906's measurement of the ratio of hydrogen to deuterium cross sections (arbitrarily plotted at 1) compared with the E866 measurements of the same quantity (left). The statistical uncertainty of E906's measurement of the ratio of deuterium to Calcium cross sections (arbitrarily plotted at 1) compared with previous Drell-Yan and deep inelastic scattering (DIS) measurements (right).

D. ATOMIC TRAP TRACE ANALYSIS

d.1. Improvements on Detecting $^{81,85}\text{Kr}$ with ATTA (K. Bailey, X. Du, Z.-T. Lu, P. Mueller, T. P. O'Connor, and L. Young*)

We report on the refinements of the Atom Trap Trace Analysis (ATTA) setup, developed by our group for the detection of the two long-lived isotopes ^{81}Kr ($t_{1/2} = 2.3 \times 10^5$ years) and ^{85}Kr ($t_{1/2} = 10.8$ years). The ATTA method is based on selectively trapping the desired Kr isotope in a Magneto Optical Trap (MOT) and detecting it by observing its fluorescence. The principle of this method has been demonstrated by measuring the isotopic abundance of ^{81}Kr and ^{85}Kr in samples of atmospheric Kr, which is readily available in large amounts, with an overall counting efficiency of 2×10^{-7} . However, in order to allow measurements of samples extracted from ancient water or ice, where obtaining just 1 cc of Kr at STP means processing tons of material, the gas consumption rate had to be reduced substantially, i.e. the overall counting efficiency had to be increased by several orders of magnitude.

Since noble gas atoms do not permanently stick to walls, the efficiency can be increased significantly by recirculating the Kr within the vacuum chambers of the

trap system (Fig. IV-20). In 2001, we conducted tests of the Kr recirculation system. With the implementation of a two-stage recirculation system, the overall efficiency was increased by a factor of 350. We have also tested a completely sealed system by closing off the path between the Chopper and Trap chambers. The pressure of Kr gas gradually decayed in such a sealed system with a half-life of 6 hours. This decay of pressure only happened when the discharge source was on, which led us to postulate that the Kr atoms were ionized and implanted into the walls of the discharge source. By completing the recirculation path from the Trap to the Cooling chamber and performing the measurement for 6 hours, the efficiency is expected to increase by another order of magnitude. With a final overall efficiency in the range of 10^{-4} to 10^{-3} , the system will be ready for dating groundwater samples due to arrive later this year.

*Chemistry Division, ANL

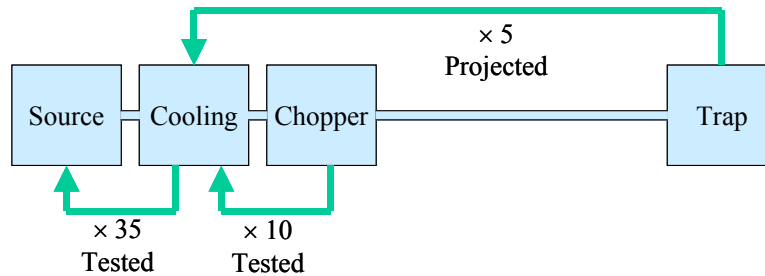


Fig. IV-20. Krypton sample recirculation system. The trap system consists of four vacuum chambers: Source, Cooling, Chopper, and Trap. Three turbopumps, attached to the downstream three chambers, are used to pump the sample gas back to the Source.

d.2. Ultrasensitive Isotope Trace Analysis of ^{41}Ca (K. Bailey, Z.-T. Lu, I. D. Moore, P. Mueller, T. P. O'Connor, and L. Young*)

An Atom Trap Trace Analysis (ATTA) system based on the technique of laser manipulation of neutral atoms is being developed to measure the isotopic abundance of ^{41}Ca in natural samples. ^{41}Ca has a half-life of 1.03×10^5 years and a natural isotopic abundance of $\sim 10^{-15}$. Trace analysis of ^{41}Ca has promising applications in archaeological dating of ancient bones and in the biomedical research of osteoporosis.

Trapping of all stable calcium isotopes has been demonstrated. For the most abundant isotope, ^{40}Ca (97% isotopic abundance), a MOT loading rate of 3×10^{10} atoms/s has been reached at the overall capture efficiency of 1×10^{-4} . An order of magnitude increase in this efficiency is realistically expected with the implementation of two-dimensional transverse cooling to reduce the atomic beam divergence and amplify the atom flux in the forward direction.

In order to analyze the rare isotope ^{41}Ca , the system must be able to detect single atoms. In 2001, we have achieved the single-atom-detection capability (Fig. IV-21) with this setup. The observed photon count rate from a single ^{40}Ca atom is 4 kHz, while the background rate is 5 kHz. With the addition of a 671 nm diode laser that pumps the trapped Ca atoms from the metastable $3d\ ^1D_2$ level back to the ground level, the average lifetime of the atoms in the trap is increased from 20 ms to 100 ms, and the time-integrated signal-to-noise ratio of a single trapped atom has reached 18.

We have also installed a new PC-based control system to monitor and control the laser frequencies, which will enable us to quickly address different Ca isotopes and measure the ratios of their abundances. This system uses a frequency-stabilized He-Ne laser to provide a reference that is transferred to the Ti:Sapphire and diode laser using a scanning Fabry-Perot cavity.

*Chemistry Division, ANL

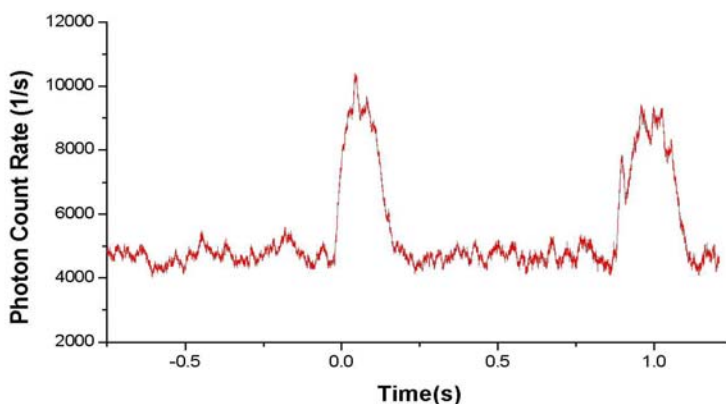


Fig. IV-21. Fluorescence signal of individual ^{40}Ca atoms in the trap.

d.3. Measuring the Charge Radius of ${}^6\text{He}$ (K. Bailey, X. Du, J. Greene, A. M. Heinz, R. J. Holt, D. Henderson, R. V. F. Janssen, C.-L. Jiang, Z.-T. Lu, I. D. Moore, P. Mueller, T. P. O'Connor, R. C. Pardo, T. Pennington, K. E. Rehm, J. P. Schiffer, G. Drake,* C. Law,† M. Paul,‡ and L.-B. Wang§)

The neutron-rich ${}^6\text{He}$ ($t_{1/2} = 807$ ms) nucleus is believed to consist of a ${}^4\text{He}$ -like core and two halo neutrons bound by less than 1 MeV. The charge radius of ${}^6\text{He}$ was predicted with the Quantum-Monte-Carlo calculations based on the Argonne v_{18} Two-Nucleon and the Illinois Three-Nucleon Potential model. This collaboration aims to determine the charge radius of ${}^6\text{He}$ by measuring the atomic isotope shift of the 2^3S_1 - 3^3P_2 transition between ${}^4\text{He}$ and ${}^6\text{He}$. Since ${}^6\text{He}$ atoms are short-lived and are available only in small numbers, we plan to produce the ${}^6\text{He}$ atoms at the ATLAS accelerator facility, capture individual ${}^6\text{He}$ atoms with a laser trap, and perform precision laser spectroscopy on the trapped atoms.

We will take advantage of the properties of Atomic Trap Trace Analysis (ATTA), which was developed by our group for the trace detection of ${}^{81,85}\text{Kr}$. This method is based on selectively trapping the atoms of the desired isotope in a magneto-optical trap (MOT) and detecting the trapped atom by observing its fluorescence. It was demonstrated that ATTA is virtually background free and is capable of detecting single atoms. The complete experimental setup will include a target chamber for on-line production of the isotopes with subsequent neutral extraction and transfer to a discharge source to produce metastable He atoms, a

Zeeman slower to decelerate the thermal beam of metastable He, a MOT with single atom detection capability and a laser system to produce the light for trapping and high resolution spectroscopy.

In 2001, we carried out two experimental runs at ATLAS. Here we report on the successful production, extraction, and detection of thermal neutral ${}^6\text{He}$ atoms. In this experiment (see Fig. IV-22), ${}^6\text{He}$ was produced via the ${}^{12}\text{C}({}^7\text{Li}, {}^6\text{He}){}^{13}\text{N}$ reaction and stopped in a porous graphite target, from which the atoms diffused out. The atoms were then compressed by a turbo-pump system, with an approximately 50% efficiency, into a small vacuum chamber where approximately 5% of the β particles from the decays of ${}^6\text{He}$ were detected by a plastic scintillation detector. We verified that the observed β particles were indeed emitted by ${}^6\text{He}$ based on the measured energy spectrum and the half-life of the β emission. From these measurements, we derived that, with a ${}^7\text{Li}$ beam current of 20 pA, ${}^6\text{He}$ atoms were extracted from the target chamber at a rate of $3 \times 10^5/\text{s}$. A factor of 10 increase in the extraction rate can be achieved at ATLAS by increasing the ${}^7\text{Li}$ beam current. The construction of the trapping setup including the laser system is currently under way.

*University of Windsor, Canada, †Monmouth College, Illinois, ‡Hebrew University, Israel, §ANL and University of Illinois-Urbana

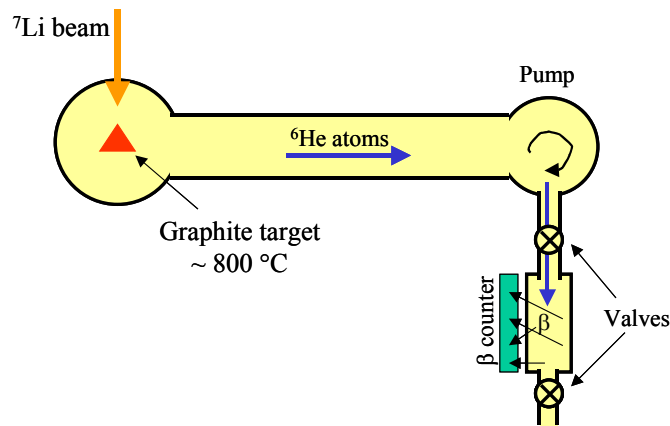


Fig. IV-22. The production, extraction, detection of neutral ${}^6\text{He}$ atoms.